



THE UNIVERSITY OF TENNESSEE

DEPARTMENT OF MECHANICAL
AND AEROSPACE ENGINEERING

A STUDY OF CONVECTIVE INERTIA
EFFECTS AND METHODS OF CONTROLLING GAS
INGESTION IN LARGE DIAMETER VISCOSEALS

by
Lawrence Howard Gutfreund

March 1970

Knoxville, Tenn 37916

This document has been approved for public release
and sale its distribution is unlimited

11-170-36776
(ACCESSION NUMBER)
(THRU)
1
(CODE)
13
(CATEGORY)
CR-12675
(PAGES)
(NASA CR OR TMX OR AD NUMBER)

FACTORY FORM 602

Reproduced by
NATIONAL TECHNICAL
INFORMATION SERVICE
Springfield Va. 22151

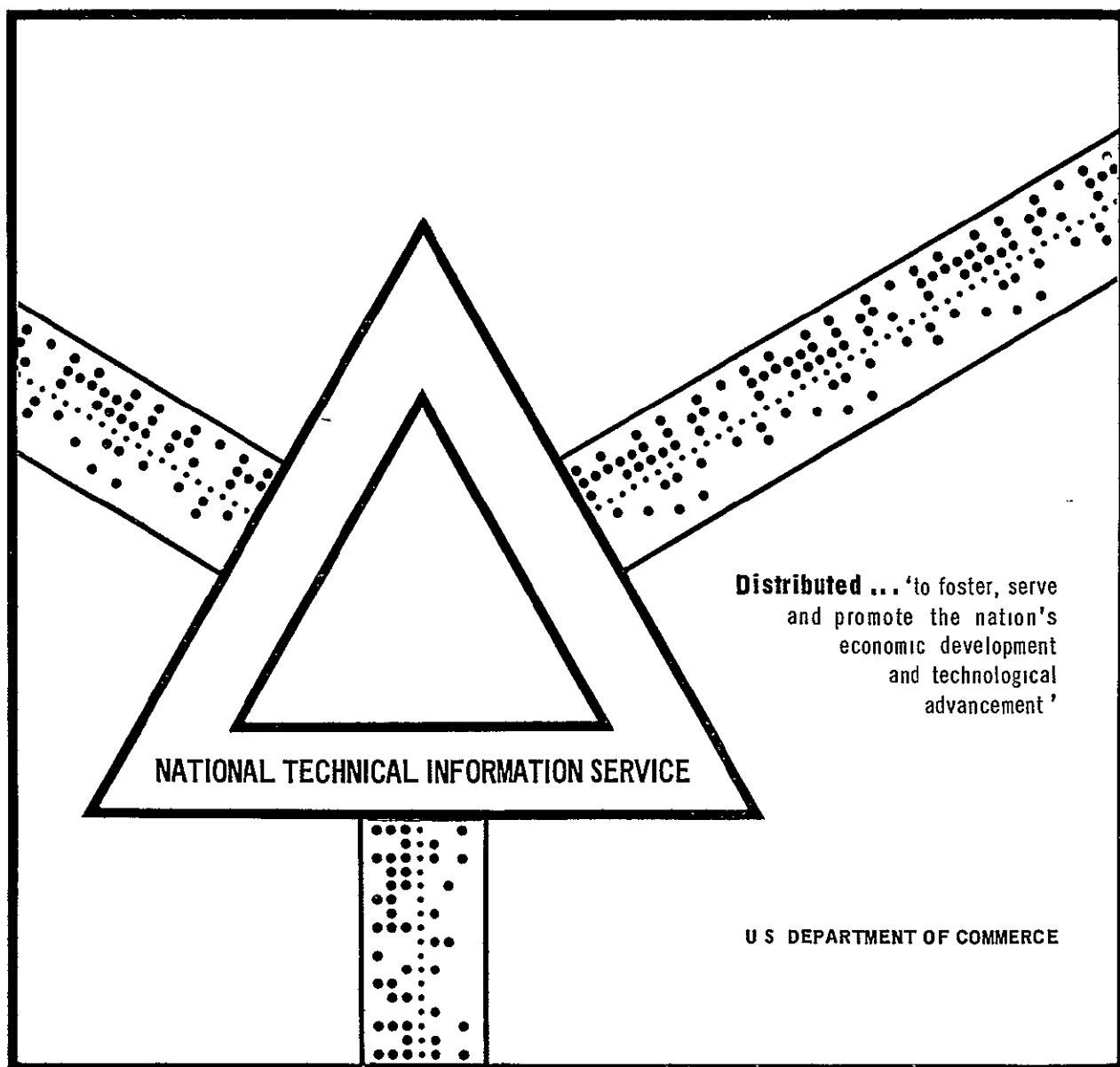
N70-36776

A STUDY OF CONVECTIVE INERTIA EFFECTS AND
METHODS OF CONTROLLING GAS INGESTION IN LARGE
DIAMETER VISCOSEALS

Lawrence Howard Luttrull

University of Tennessee
Knoxville, Tennessee

March 1970



The University of Tennessee
Department of Mechanical and Aerospace Engineering

A STUDY OF CONVECTIVE INERTIA EFFECTS AND
METHODS OF CONTROLLING GAS INGESTION
IN LARGE DIAMETER VISCOSEALS

by
Lawrence Howard Luttrull

Supported by
NATIONAL AERONAUTICS AND SPACE ADMINISTRATION
DEPARTMENT OF DEFENSE

Prepared Under
NASA Grant NGR-43-001-003

<p>This document has been approved for public release and sale, its distribution is unlimited</p>

March 1970
Knoxville, Tennessee 37916

FOREWARD

This document is submitted as an interim report on the viscoseal which is part of the University of Tennessee Dynamic Sealing research program. Support for this work was provided by contract N00014-68-A-0144 with the Office of Naval Research and grant NGR-43-001-003 from the National Aeronautics and Space Administration.

This report was submitted to the University of Tennessee in partial fulfillment of the requirements for the degree Master of Science and is presented here with minor changes in format.

The author wishes to express appreciation to Dr. C. F. Fisher and Professor W. K. Stair of the Department of Mechanical and Aerospace Engineering for their assistance in the preparation of this report.

Approved


Task Director


Lawrence Howard Luttrull

Approved


W. K. Stair
Program Manager
Project THEMIS

ABSTRACT

This study is concerned with the effect of two parameters, characteristic length and aspect ratio, on the performance of large diameter viscoseals, and with methods of preventing or controlling gas ingestion in the same device.

The characteristic length, or length of the groove-land pair in the direction of seal rotation and the aspect ratio, or ratio of groove width to groove depth, arose as parameters likely affecting viscoseal performance in a viscoseal analysis by Zuk, Ludwig, and Johnson (1) who included the convective inertia terms heretofore neglected or only indirectly included in other analyses. Two series of three seals each were tested to determine the effect of each parameter on performance. One series of seals varied only characteristic length and aspect ratio, and the other series varied only characteristic length and γ . Results showed that the characteristic length had a negligible effect on viscoseal performance. The aspect ratio affected performance in the transition region where a higher aspect ratio produced a lower transition Reynolds number.

Two methods of controlling or preventing gas ingestion in viscoseals were studied. One, the centrifugal separator, sets up a circulating flow loop in the upper half of the viscoseal which sweeps gas bubbles into an inner cavity where they are separated out to the gas side of a liquid-gas interface while the fluid returns to the annulus. The centrifugal separator was designed into a viscoseal which had already been tested for performance and gas ingestion rate. Results showed that the separator reduced gas accumulation in the sealed cavity by an order of magnitude while further modification resulted in an additional reduction of about 30% to 40%. The separator had a negligible effect on sealing performance as measured by a sealing coefficient.

Another method of controlling ingestion involved a backflow of fluid from the high pressure to the low pressure end of the viscoseal. Results showed that a backflow of suitable magnitude would effectively sweep out ingested gas and prevent its transport to the high pressure end of the viscoseal.

TABLE OF CONTENTS

CHAPTER	PAGE
I INTRODUCTION	1
Convective Inertia Effects	1
Gas Ingestion	4
II LITERATURE SURVEY .	7
Convective Inertia Effects	7
Aspect Ratio .	9
Gas Ingestion	10
III APPARATUS AND PROCEDURE	16
Inertial Test Apparatus .	16
Inertial Test Procedures	20
Ingestion Test Apparatus .	22
Ingestion Test Procedures .	25
IV RESULTS AND CONCLUSIONS	26
Inertial Test Results	26
Ingestion Test Results	31
Backflow Test Results .	40
Conclusions	43
BIBLIOGRAPHY	45
VITA	48

LIST OF FIGURES

FIGURE	PAGE
1 Elements of a Typical Viscoseal	2
2 Centrifugal Separator	6
3 Boon's Viscoseal with Recirculation of Ingested Air	14
4 Assembled Test Apparatus	17
5 Photo Showing the Assembled Test Apparatus with Seal 12-A Mounted on the Shaft	18
6 Photo Showing the Complete Test Facility	18
7 Illustration of Viscoseal Dimensions	19
8 Q Versus k for Centrifugal Separator	24
9 Experimental Performance of Seals 11, 14, 15	27
10 Experimental Performance of Seals 11, 12, 13	28
11 Seal 12-C at $Re_c = 770$ (900 rpm), $T = 71^\circ$ F, Operating with Water	33
12 Seal 12-C at $Re_c = 1560$ (1800 rpm), $T = 72^\circ$ F, Operating with Water	33
13 Seal 12-C at $Re_c = 2000$ (2200 rpm), $T = 82^\circ$ F, Operating with Water	33
14 Temperature, Pressure, and Accumulated Air Versus Time for Seal 12-C at 3600 rpm	35
15 Seal 12-C Within One Minute of Operation at 3600 rpm, $T = 71^\circ$ F, Operating with Water	37
16 Seal 12-C at 3600 rpm, $t = 5$ min, $T = 95^\circ$ F, Operating with Water	37
17 Seal 12-C at 3600 rpm, $t = 10$ min, $T = 112^\circ$ F, Operating with Water	37
18 Seal 12-C at 3600 rpm, $t = 15$ min, $T = 125^\circ$ F, Operating with Water	38
19 Seal 12 Within One to Two Minutes of the Beginning of Operation at 3600 rpm, $T = 75^\circ$ F, Operating with Water	38
20 Experimental Performance of Seal 12-A	41
21 Experimental Performance of Seal 12-C	42

LIST OF SYMBOLS

SYMBOL	DESCRIPTION	UNITS
<u>English Alphabet</u>		
a'	Land width normal to the grooves	inch
b'	Groove width normal to the lands	inch
c	Radial clearance	inch
D	Seal diameter	inch
h	Groove depth	inch
k	Axial seal length from the interface to the top of the rotor	inch
L	Active seal length	inch
L^*	Characteristic length = $(a' + b')\csc \alpha$	inch
n	Number of thread starts	
P	Pressure	$\text{lb}_f/\text{inch}^2$
Q	Mass flow rate	lb_m/sec
Re_c	Reynolds number based on radial clearance	
Re_{c+h}	Reynolds number based on radial clearance plus groove depth	
Re_h	Reynolds number based on groove depth	
Re_{crit}	Reynolds number at which transition from laminar to turbulent operation occurs	
Re	Modified Reynolds number based on characteristic length	
t	Time	minutes
T	Temperature	degrees F
U	Surface velocity of rotor	inches/sec
u, v, w	Velocity components	inches/sec
x, y, z	Coordinates	inch

Greek Alphabet

α	Helix angle	degrees
β	$(h + c)/c$	
γ	$b'/(a' + b')$	
Λ	Sealing coefficient = $6\mu UL/c^2 \Delta P$	

LIST OF SYMBOLS, continued

SYMBOL	DESCRIPTION	UNITS
μ	Absolute viscosity	$\text{lb}_f \text{sec}/\text{inch}^2$
ν	Kinematic viscosity	centistoke
ρ	Density	$\text{lb}_m/\text{foot}^3$
σ	Surface tension	dyne/cm
ω	Angular velocity	radian/sec

CHAPTER I

INTRODUCTION

This thesis is concerned with the effect of two parameters, characteristic length and aspect ratio, on the performance of large diameter viscoseals, and with methods of preventing or controlling gas ingestion in the same device.

1. Convective Inertia Effects.

The viscoseal (also called viscosity pump, threaded seal, spiral groove seal, or helical groove fluid film seal) is a dynamic shaft seal which generates an axial pressure gradient in a viscous fluid enclosed in an annular space between a rotor and housing. Helical grooves, located on the rotor or the housing or both, pump the viscous fluid and create the axial pressure gradient. This device acts as a pump with a net efflux of fluid at the high pressure end or as a seal when operating at shut-off head. A typical viscoseal is shown in Figure 1.

The viscoseal was first studied as a pump and later as a seal as the need for reliable, long life, low leakage seals in demanding engineering situations arose. The viscoseal is suited for such situations since it does not depend on rubbing contact for effective operation, it has low wear rates, and it has essentially zero leakage rates.

A number of relations have been presented for predicting viscoseal performance under laminar conditions (3,4,5,11) and a fewer number for turbulent conditions (5,6,7,8), some of which are discussed in the literature survey which follows. The various laminar equations are similar in that performance is characterized by some sealing coefficient of the general form $\Lambda = 6\mu UL/c^2 \Delta P$ (2). The predictions of Λ as a function of seal geometry differ as do predictions of optimum seal geometry. These analyses assume convective inertia forces to be negligible as compared to viscous forces, and otherwise assume steady, isothermal, incompressible, laminar flow

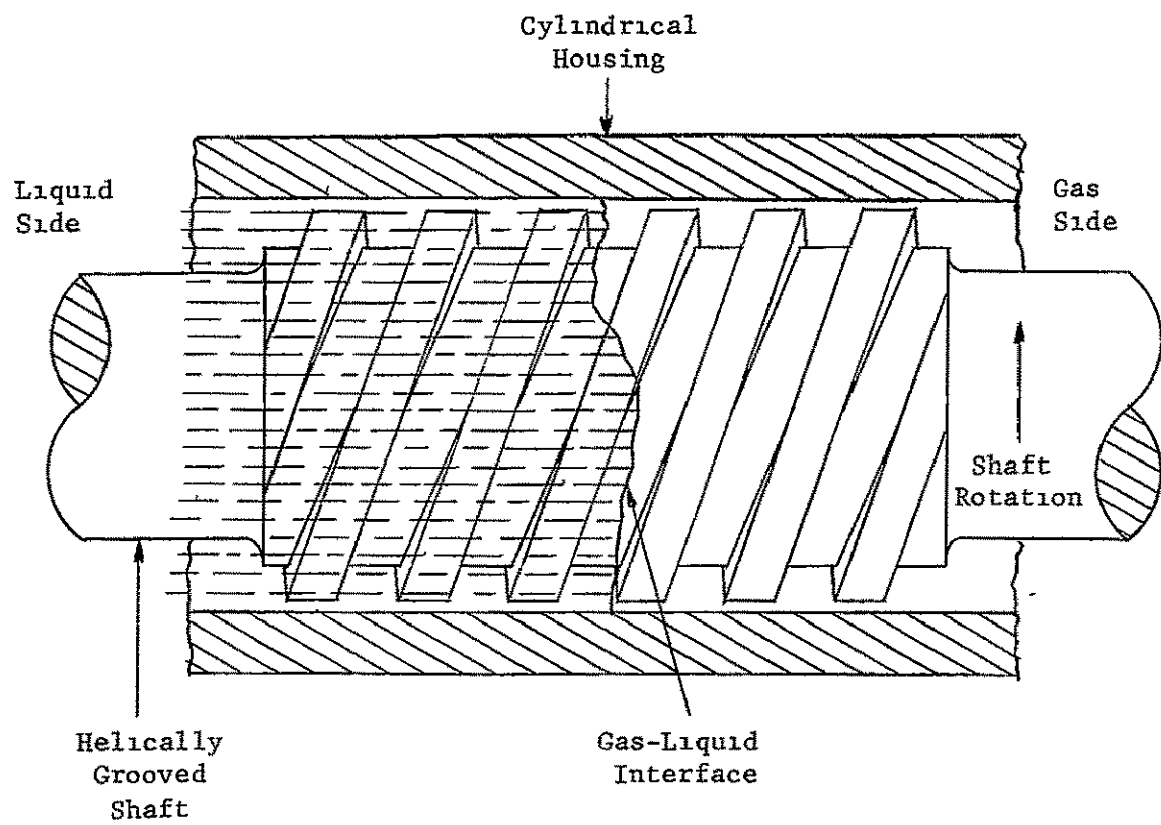


Figure 1 Elements of a typical viscoseal

Experimentally the sealing coefficient is constant for low Reynolds numbers ($Re_c \leq 200-600$) which is normally termed the laminar or creeping flow regime. At high Reynolds numbers, the sealing coefficient improves with increasing Reynolds number. This regime has been termed turbulent and the improvement in sealing has been attributed to the onset of turbulence. Between the laminar and turbulent regimes is the transition region which presents a smooth change from a steady to a varying sealing coefficient. The start of transition has normally been predicted by a critical Reynolds number which is a function of seal geometry, but transition has been hard to predict with any precision.

The turbulent analyses are somewhat dissimilar in that most investigators take different approaches to including effects of turbulence. They are similar in that most investigators do assume turbulence to be present. They either neglect the effect of convective inertia forces or include them indirectly through the use of empirical coefficients.

Convective inertia is an acceleration of fluid mass due to a spatial velocity change such as a change due to an obstacle in the flow path. The convective acceleration terms appear in the Navier-Stokes equations in the Eulerian or spatial derivative D/Dt which also includes the local or temporal acceleration. Thus

$$D/Dt = \underbrace{\partial/\partial t}_{\text{Temporal Acceleration}} + \underbrace{u\partial/\partial x + v\partial/\partial y + w\partial/\partial z}_{\text{Convective Acceleration}}$$

In an analysis by Zuk, Ludwig, and Johnson (1), the convective inertia terms were included in a unified approach to laminar and turbulent operation. From their analysis evolved a modified Reynolds number Re^* which was based on the characteristic length L or the length of the groove-ridge pair in the direction of rotation of the seal. Thus

$$Re^* = (UL/\nu)(c/L)^2 = \text{inertia forces/viscous forces}$$

Applying this concept to experimental results, they found that departure from a constant sealing coefficient, which others claimed to be due to the onset of turbulence, took place at a Re^* value of approximately one. They conclude that this improvement in the sealing coefficient is due to the onset of significant convective inertia force

Since most experimental studies of viscoseals have utilized seals with diameters of two inches or less and a limited number of thread starts, the values of L have varied over a limited range. Therefore, a series of three large diameter seals, geometrically similar except for their characteristic lengths and aspect ratios, were tested.

The consideration of convective inertia forces in viscoseal analysis revealed parameters affecting viscoseal performance that were heretofore neglected by most analyses. The most significant of these is the aspect ratio b'/h , the ratio of groove width to groove depth. Zuk stated that the aspect ratio implies the degree of the convective inertia effect and could therefore not be neglected unless its value is quite large. Most analyses neglect the aspect ratio because of its large magnitude. A series of three viscoseals with equal aspect ratios was assembled and was tested and compared with the previously mentioned three seals to reveal the effect of aspect ratio on sealing performance.

2 Gas Ingestion

In the testing of viscoseals, a serious problem arose whereby gas bubbles passed through the liquid-gas interface and were transported to the high-pressure end of the seal. This phenomenon has been termed gas ingestion and in severe cases can lead to a leakage of sealed fluid. Gas ingestion has become the subject of increasing study although it is still not understood how gas bubbles are transported against an adverse pressure gradient to the high-pressure end of the seal. A study of the stability of a dynamic gas-liquid interface between rotating cylinders made by Fisher (9) has revealed a mechanism by which gas can be ingested at the interface. Other studies (5,8) have revealed possible correlations between the onset of ingestion and various nondimensional numbers (Reynolds, Weber, Froude, Cavitation), and many parameters which affect ingestion have been revealed. However, as Fisher concludes, gas ingestion in viscoseals is an essentially inherent phenomenon which cannot readily be eliminated through optimization of the viscoseal geometry.

Thus, a means of controlling existing ingestion and preventing its being transported to the sealed cavity rather than preventing ingestion altogether might be the proper mode of handling the ingestion problem

A concept of recirculating entrained gas was introduced by Boon (10) Radial passages connected to an inner axial passage allowed gas bubbles to be recirculated to the upper part of the annulus However, the change of geometry of the seal required to completely stop gas transport also adversely affected the sealing coefficient

Following this work, Fisher designed a centrifugal separator into a viscoseal that would circulate gas bubbles and liquid into an inner cavity, separating the gas bubbles out to the gas side of the fluid layer in the cavity and returning the liquid to the annulus An existing viscoseal, whose performance already had been measured, was modified, as shown in Figure 2, to study the effectiveness of the principle

Another method of controlling and possibly eliminating ingestion was investigated This method involved a backflow of fluid against the pumping action of the viscoseal in order to sweep out existing air bubbles and prevent their transport through the annulus This method is impractical due to the fact that it completely defeats the purpose of the seal and produces significant leakage rates However, it was thought that it might provide some insight into the mechanism of gas transport or lend itself to other possible methods of controlling gas ingestion

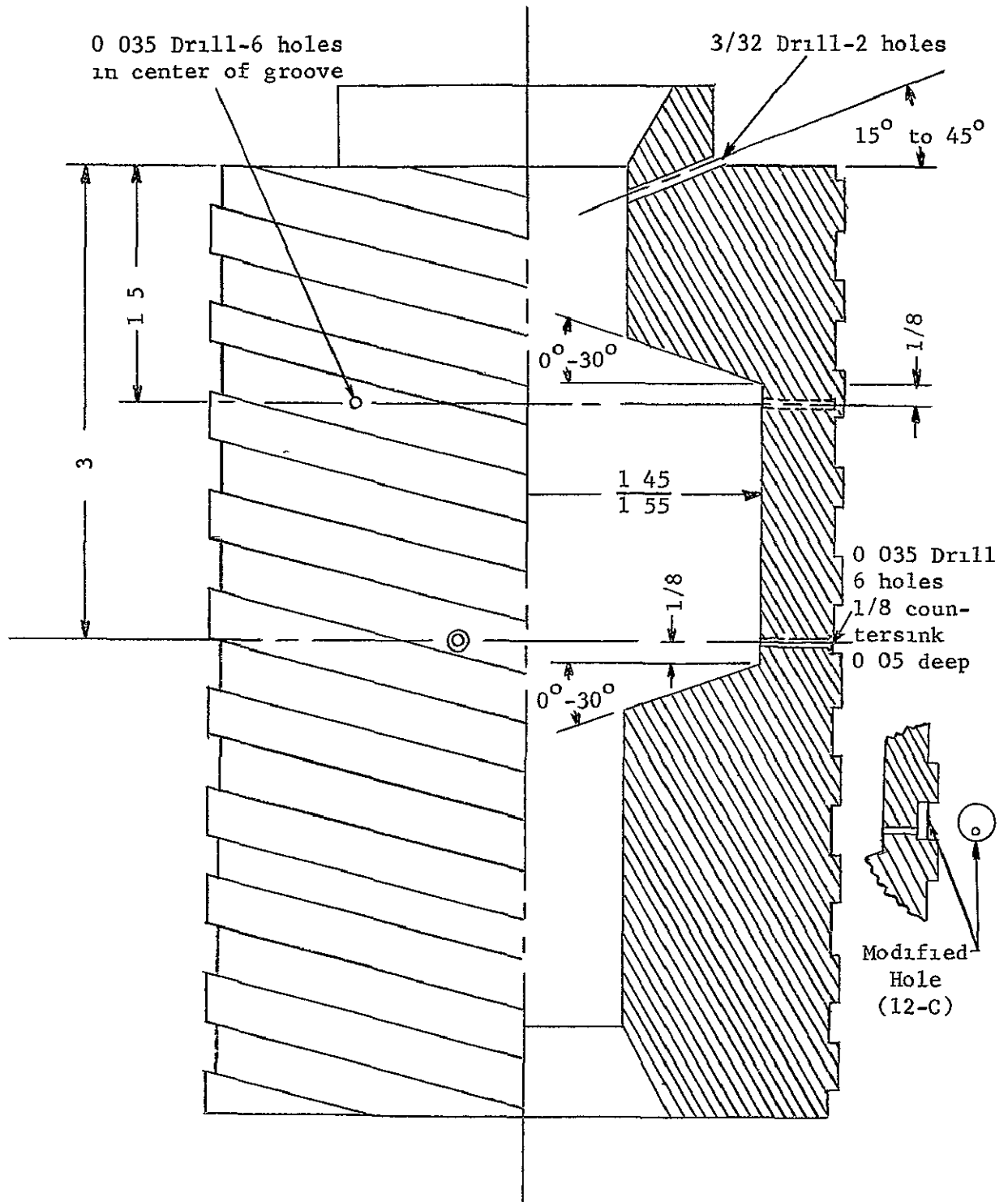


Figure 2 Centrifugal separator

CHAPTER II

LITERATURE SURVEY

1 Convective Inertia Effects.

A survey of literature on viscoseals reveals that convective inertia effects normally are either neglected in a laminar or creeping flow analysis, or they are indirectly introduced through the use of empirical coefficients in an analysis which treats the turbulent operation of the viscoseal. A significant improvement in sealing coefficient is attributed to the onset of turbulence which is predicted by a critical Reynolds number. As the Reynolds number becomes small, the analysis approaches that of laminar or creeping flow.

McGrew and McHugh (5) introduced inertia forces into their turbulent analysis by using Prandtl's mixing length. This concept uses an empirical factor that must be determined by experiment. The result was an equation of the form $\psi = K_1 + K_2(Re_h)^n = 6/\Delta$ where K_1 , K_2 , and n are experimentally determined and K_1 is the laminar value of ψ .

King (8) also incorporated inertia forces indirectly using, in part, the form of the McGrew and McHugh equation. He proposed an equation of the form $\Delta p c^2 / \mu \omega L d = K_1 (Re_h / K_2)^n$ and found the values of K_1 , K_2 , and n from experimental data where again K_1 is the value of the laminar sealing coefficient.

Pape and Vrakking (7) indirectly included inertia effects since certain empirical coefficients were obtained by use of turbulent flow correction coefficients presented by Ng and Pan.

Stair and Hale (6) used empirical coefficients determined from pipe friction data in their turbulent analysis. They further predicted the onset of turbulence at a critical Reynolds number defined as

$$Re_{crit} \leq 41 \left[(D/2) / ((1-\gamma)c + \gamma Bc) \right]^{\frac{1}{2}}$$

This equation is based on the Taylor criterion for the onset of turbulence in concentric cylinders with the inner cylinder rotating. Experimentally they found the onset of turbulence at lower Re_c .

values as γ increased in tests with the same α and β . They also found that the onset point began at lower Re_c values for increasing α .

Schlichting (12) treated the relative magnitudes of viscous and inertia forces in connection with the hydrodynamic theory of lubrication. In his treatment of flow in a wedge between slide block and plane guide surface, he used a reduced Reynolds number Re' to give the relative importance of viscous and inertia forces where

$$Re' = \text{Inertia force/Viscous force} = (\rho u du/dx) / (\mu d^2u/dy^2) = (\rho u^2/L) / (\mu u/h^2) = (\rho u L / \mu) (h/L)^2$$

Here, h is the distance between slide block and guide surface and L is the length of the slide block in the x -direction.

Zuk, Ludwig, and Johnson (1) presented the only unified approach covering both laminar and turbulent operation of the viscoseal. They formulated a set of two-dimensional equations that directly included both viscous and inertia forces. The equations can be solved using numerical methods on a high speed digital computer. A modified Reynolds number, Re^* , similar to that presented by Schlichting, evolved from a formal ordering procedure applied to the conservation of mass and momentum equations. It was based on the characteristic length L , which is the length of the groove-ridge pair in the direction of rotation of the seal. As Schlichting stated, the convective inertia forces can be neglected only when this Reynolds number is much less than one. As mentioned previously

$$Re^* = \text{Inertia force/Viscous force} = (UL/\nu)(c/L)^2$$

Zuk, Ludwig, and Johnson applied the modified Reynolds number concept to the published experimental results of four researchers. The departure from a constant sealing coefficient, an occurrence normally attributed to the onset of turbulence, occurred in a range of Re^* values of 0.26 to 2.2 or, in other words, when Re^* was near unity. This result suggests that what others predicted to be the beginning of turbulence was actually the beginning of significant convective inertia effects which cause an improvement in the sealing coefficient. This improvement was further attributed to the fact that the axial pressure gradient results from an unbalance of convective inertia force and drag force across the groove-ridge pair.

Zuk, Ludwig, and Johnson further noted the work of Kettleborough (13) who numerically analyzed the slider bearing with inertia, turbulent, and viscous terms considered. When he considered only inertia terms in his analysis, the results were in qualitative agreement with published, turbulent-attributed, slider bearing experimental results. He concluded that the turbulent terms did not greatly affect the operation of the slider bearing.

2 Aspect Ratio

Zuk, Ludwig, and Johnson's consideration of convective inertia effects (1) revealed parameters affecting viscoseal performance that are somewhat neglected by other authors. Most notable is the aspect ratio, the ratio of groove width to groove depth, which implies the degree of the convective inertia effect. They state that the physical significance of the aspect ratio is the fact that it is the distance over which the fluid accelerates and then decelerates on impact with the ridge edge. Since this edge causes convective acceleration, its effects are not negligible unless the aspect ratio is very large. As the ratio increases, the point of improvement in sealing coefficient or onset of inertia forces occurs at lower Re_c values. This is explained by the reasoning that a larger ridge area or low aspect ratio results in a less influential convective inertia effect and delays the beginning of significant inertia effects.

In the analyses of most authors (6,7,14), the assumption is made or implied that the aspect ratio is so large as to be insignificant. This was found to be evident particularly in turbulent analyses.

However, some authors mentioned aspect ratio to some degree. Rowell and Finlayson (15), in their analysis on the viscosity pump, showed that both the ideal flow rate and the maximum pressure developed increased as aspect ratio increased. They experimentally observed that for values of aspect ratio greater than two, the calculated and experimental results were in good agreement.

In his analysis of the laminar viscoseal, Asanuma (4) showed that for a smaller groove depth or larger aspect ratio, a better sealing coefficient resulted for a zero clearance seal. For a

finite clearance, the optimum sealing coefficient was obtained at aspect ratios of five to twenty

Weinand and Wroblewski (16) conducted experimental tests on a series of viscoseals that were identical except for the groove depth. They found that the aspect ratio giving a maximum pressure generation was small for low viscosity sealing fluids and larger for higher viscosity sealing fluids. In general, they found the optimum ratios to lie between 3.3 and 16.7

3 Gas Ingestion

The problem of gas being ingested into a sealing fluid through the liquid-gas interface has been observed and reported by a majority of those who have experimentally studied the viscoseal. Some researchers have focused their studies on gas ingestion alone with some insight being gained into the basic causes of the problem. Furthermore, several partial solutions to the ingestion problem have been proposed and tested with varying degrees of success.

Several authors (3,17,18,19,20) have simply reported gas ingestion in viscoseal operation. In each case a drop in pressure generation was observed at high speeds along with foam generation or the appearance of a liquid-gas mixture in the seal. The ingestion was found in both grooved rotor-smooth housing and grooved housing-smooth rotor combinations. In some cases pressure generation ceased entirely, and in some cases a leakage of sealing fluid was reported.

King (8) made a closer study of a "secondary leak" in his vertically mounted viscoseal with the sealed fluid above the grooved rotor. He reported the leakage as varying with speed and clearance and thought that it depended also on the Weber number (the ratio of inertia forces to surface tension forces), the Froude number (U^2/gc), and the location of the liquid-vapor interface. The results were obtained with water and potassium.

McGrew and McHugh (5) also made a study of "seal breakdown" on a vertically placed viscoseal with fluid above the grooved rotor. The "seal breakdown" was a breakdown in the sealing capability upon reaching a certain speed and yielded a leak of about one drop every three minutes. The seal pressure also dropped. They concluded that

cavitation did not seem to be the cause since it was possible to run with water at values of cavitation number far below one. Nor did gravitational force seem important since the Froude number would indicate that breakdown would always occur at the same shaft speed, which was not the case. The Weber number data presented a more consistent pattern since in three of the four fluids used, breakdown occurred in the range of Weber numbers of 800 to 1100. It also appeared that fluids with high values of surface tension to density ratio could be operated at higher velocities without breakdown.

Ludwig, Strom, and Allen (21) investigated ingestion in both grooved rotor and grooved housing situations with the housing being transparent for observation. They reported the onset of ingestion at a Re_{c+h} value of 2300 using a grooved rotor and water. The ingestion increased in rate with increasing Re_{c+h} . In tests with a grooved housing and smooth rotor, ingestion began at $Re_{c+h} = 2300$, but at $Re_{c+h} = 8400$ and higher, no ingestion was evident. In each case the maximum Re_{c+h} value was 13,000 (12,000 rpm). They reasoned that in the grooved housing case, the air bubbles were displaced to the smooth rotor surface by centrifuge action where they could pass over the lands and not be pumped to the high pressure end of the seal. With a grooved rotor, the air bubbles were displaced into the grooves and pumped to the sealed cavity. When the air in the cavity formed a bubble that reached the size of the rotor outer diameter, the gas blew back out the annulus. If the interface was far enough from the low pressure end of the seal, the liquid forced out by the blowing gas would be scavenged back into the seal and no leak would occur. These results were observed in both water and sodium. Ludwig, Strom, and Allen also observed that the size of air bubbles decreased in moving from the low to the high pressure end of the seal. They stated that it is probable with longer seal lengths and corresponding high pressures to be able to reduce the bubble size enough to allow escape over the lands and thus eliminate ingestion.

Stair (2) also studied gas ingestion in a horizontally placed viscoseal using water as the sealing fluid. He observed the onset of ingestion at certain speeds and an increase with increasing speed. In some cases a speed was reached at which the pressure profile became unstable and rather severe pulsations occurred. Continued operation was characterized by pulsating leak. The seal did not otherwise leak unless the effective seal length required to maintain sealant supply pressure became longer than the active seal length. Evidence indicated that ingestion increased with eccentric seal operation and was reduced by wide grooves and narrow lands. Ingestion was not observed in one seal which had narrow lands and a large helix angle. Furthermore, ingestion was more severe and began at lower speeds when the seal surface was completely wetted by the fluid. Nonwetting was achieved by coating the surface with oil.

In another report (22), Stair described the operation of three seals with small clearance dams on each end of the grooved section of the viscoseal shaft in order to reduce ingestion. Although not as effective as expected, the dams did slightly decrease ingestion without affecting the sealing coefficient.

Fisher (9) made a stability analysis of a dynamic gas-liquid interface such as exists in a viscoseal using the same test facility as used for this thesis. He used smooth rotors inside smooth, transparent housings. He found that " gas entrainment can result from a gas-liquid interface instability caused by a velocity of a portion of the interface toward the more viscous fluid and/or an acceleration of a portion of the interface toward the more dense fluid ". He further credited eccentricity, shaft runout, and vibration with contributing to interface instability while fluid surface tension would tend to stabilize the interface and prevent or delay ingestion. He found no significant relation between the beginning of air entrainment and the Weber number or the Reynolds number or combinations of the two. While Fisher's study did not reveal the method with which gas bubbles are transported to the high pressure end of the seal, it did provide an " explanation of a possible mechanism by which gas ingestion can occur in the region of a gas-liquid interface "

Zuk, Strom, Ludwig, and Johnson (23) also observed that shaft runout and eccentricity caused axial and circumferential oscillations of the gas-liquid interface. The region of liquid-gas mixture and the gas ingestion were more severe than with low runout, concentric operation. They also reported that vibration appeared to affect the interface.

A rather extensive study of gas ingestion and the prevention of gas ingestion was made by R J G. Boon (10). Using a vertically mounted viscoseal with grooved rotor and a transparent housing, Boon confirmed many of the observations of Stair and Ludwig, Strom, and Allen concerning the onset and build-up of ingestion. He used a fluid which was a 1:5 mixture of Tellus 11 and "Petrol". The fluid had a kinematic viscosity of 1.94 centistokes at 69° F. He reported no ingestion at the lowest speed of 1082 rpm along with a well defined oil-air interface. Any gas previously under the cylinder slowly disappeared at this speed. He also reported no ingestion when using two other fluids - Tellus 13 and Tellus 11 - with higher viscosities - 21.4 and 9.57 centistokes respectively - up to the maximum speed of 4120 rpm. He did expect, based on other investigator's reports, that ingestion would occur in these fluids at sufficiently high velocities.

Boon made an extensive and somewhat successful effort at preventing ingestion in the single and double viscoseal. He found that ingestion was diminished strongly by raising the liquid level well over the top of the rotor, the sealed cavity being under the rotor. He also found that deepening the grooves on the single viscoseal reduced the ingestion, particularly at lower numbers of revolutions. Ingestion was somewhat delayed from getting under the cylinder by placing a barrier ring at the high pressure end of the seal. The outer diameter of the barrier ring was equal to that of the rotor lands.

The most significant influence on gas ingestion involved the recirculation of ingested gas in the upper half of the rotor. As shown in Figure 3, a hole was drilled along the axis of the rotor. One radial channel at the upper end of the rotor and two radial

channels at the center of the rotor connect the rotor surface with the inner hole. The gas, being displaced to the rotor surface by centrifuge action, disappears into the radial channels and is then returned to the upper part of the annulus through the upper radial channel. This arrangement gave an observable decrease in the transport of gas beyond the lower radial channels.

A further modification was made by machining a 1 mm deep, 2 mm wide groove around the rotor in the plane of the two lower channels. A strong improvement was observed, but gas still passed the groove. The groove was deepened to 4 mm and the radial channels were enlarged to a diameter of 1.5 mm. Another strong improvement was noted, however, enough gas still reached the sealed cavity in 15 minutes to blow back up through the annulus.

Noting that gas transport beyond the groove could be caused by a small decrease in pressure behind the land, 5 mm of the land was machined away on each side of the groove. This geometry did not give an observable leak under any conditions as long as the liquid level was above the center groove. However, by putting the groove around the center of the rotor, the active length of the seal was cut in half, probably due to the fact that the upper half of the rotor was densely populated with gas bubbles. Therefore, the sealing coefficient was adversely affected, being reduced by about 40%. Recirculation in the double viscoseal yielded the same results.

CHAPTER III

APPARATUS AND PROCEDURE

1 Inertial Test Apparatus.

The test facility used in this study is the same as that used by Fisher in his interface stability analysis. It was designed and built to allow both visual observation of viscoelastic operation and measurement of the physical properties related to the determination of the seal performance. A sketch of the assembled rig appears in Figure 4 with photographs of the same in Figures 5 and 6.

A stainless steel shaft was designed so as to permit mounting of interchangeable aluminum test rotors from two to eight inches in diameter. The rotors were positioned on the shaft by a tapered shoulder on the shaft and by a tapered nut which fitted into the lower end of the rotors. The shaft was vertically mounted and supported at the upper end by a ball bearing and at the lower end by a helical groove hydrodynamic journal bearing. The lower bearing was lubricated by the liquid being used in the seal and was replaced when the wear on the inside surface became excessive. The shaft was driven at the upper end by a V-belt connected to a variable speed motor. The motor drove the shaft at speeds up to 3600 rpm. After the characteristic length tests, an idler was added to tighten the V-belt and reduce vibration of the shaft.

Each rotor had a nominal diameter of four inches and the length of the threaded section was six inches. The exact dimensions are listed in Table I. It is noticed that seals 11, 12, and 13 have a constant D , α , h , β , and γ with varying L and b'/h , while seals 11, 14, and 15 have constant D , α , h , β , and b'/h with varying L and γ . It was impossible to construct a series of seals which varied only L or only the aspect ratio. However, knowing the effect of γ on performance, seals 11, 14, and 15 should indicate the effect of L , and, knowing this effect, the influence of aspect ratio can be established from seals 11, 12, and 13. The runout of each seal while mounted on the shaft was measured using dial indicators. In each case the runout was less than one mil.

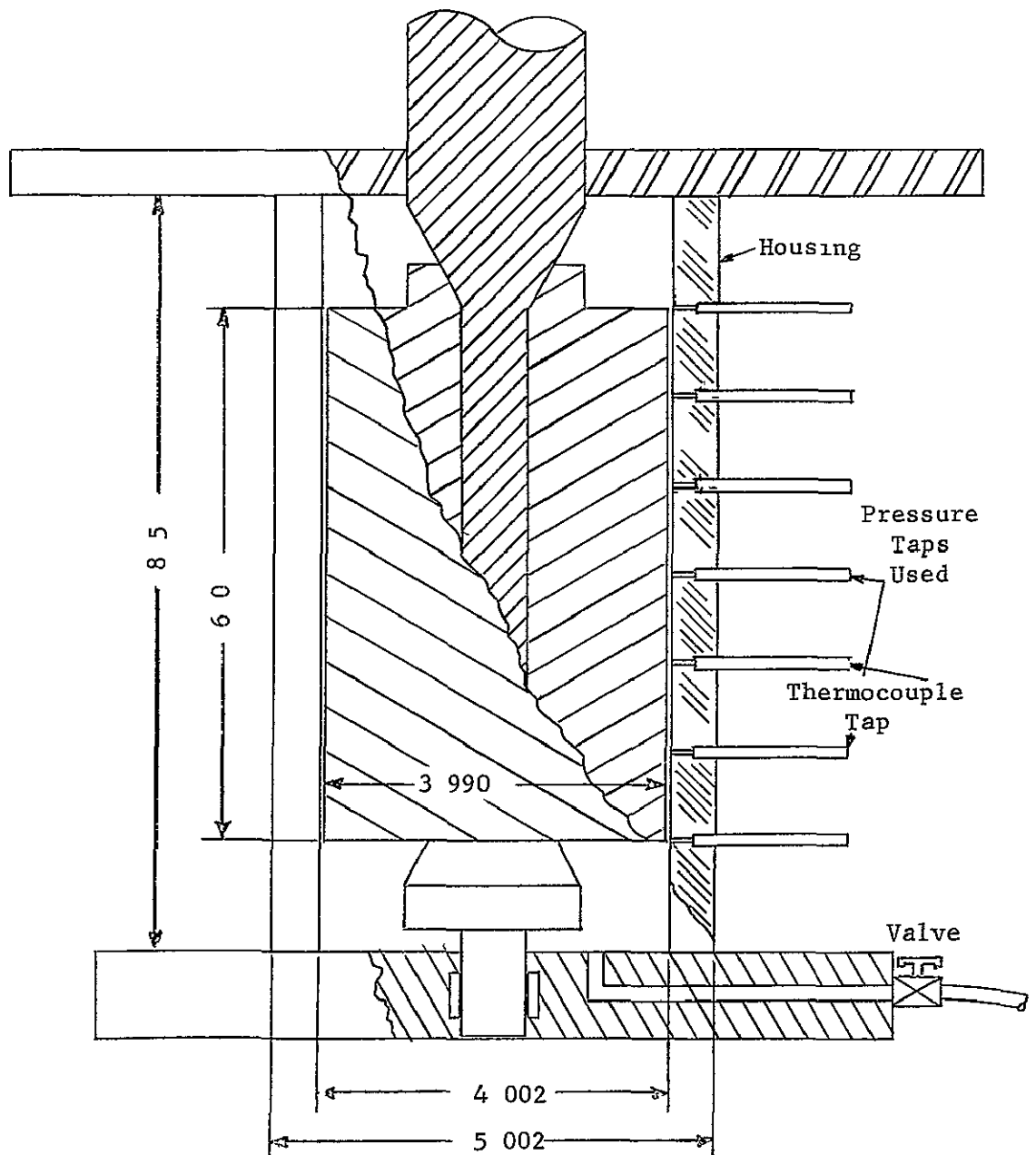


Figure 4 Assembled test apparatus

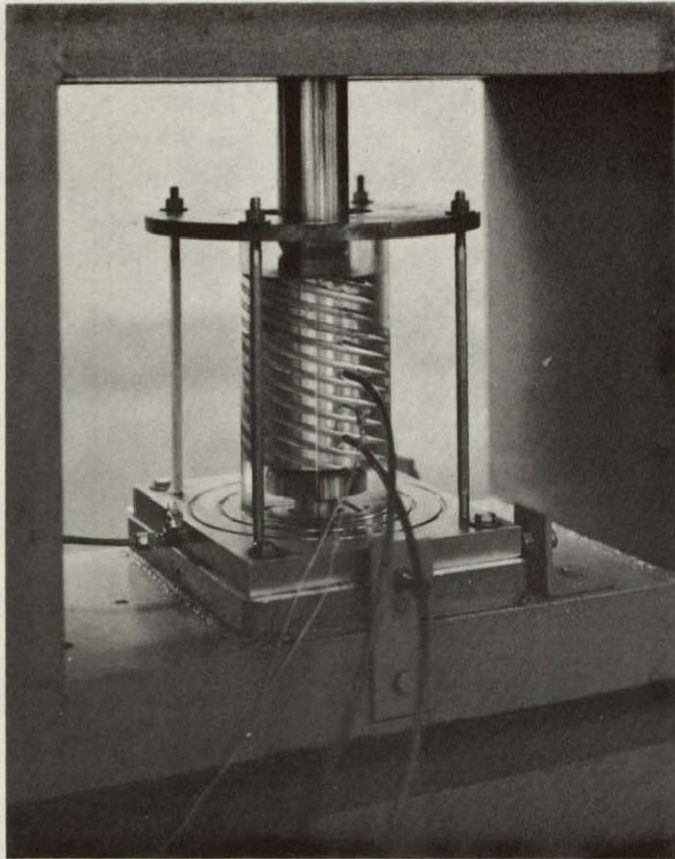


Figure 5. Photo showing the assembled test apparatus with seal 12-A mounted on the shaft.

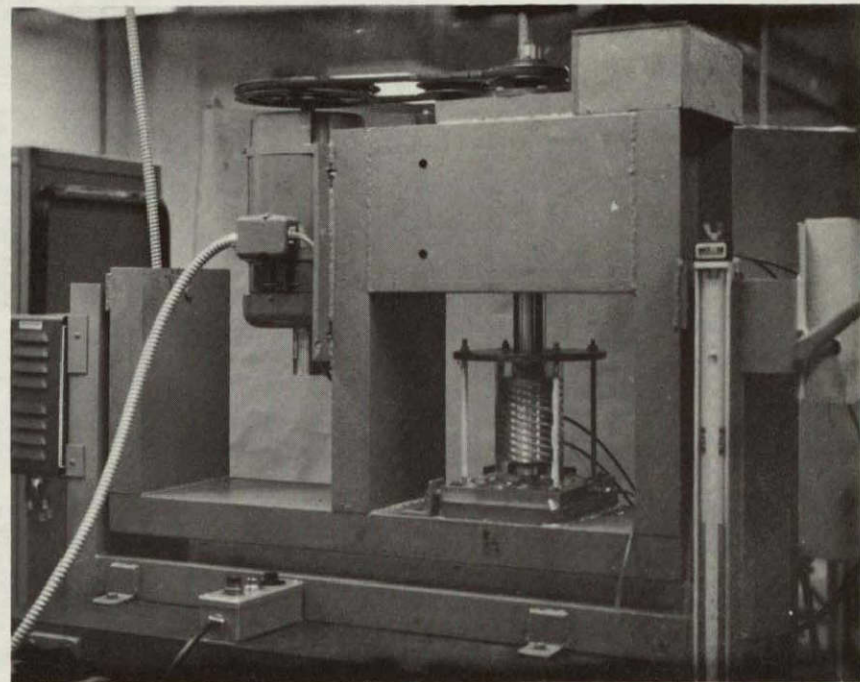


Figure 6. Photo showing the complete test facility.

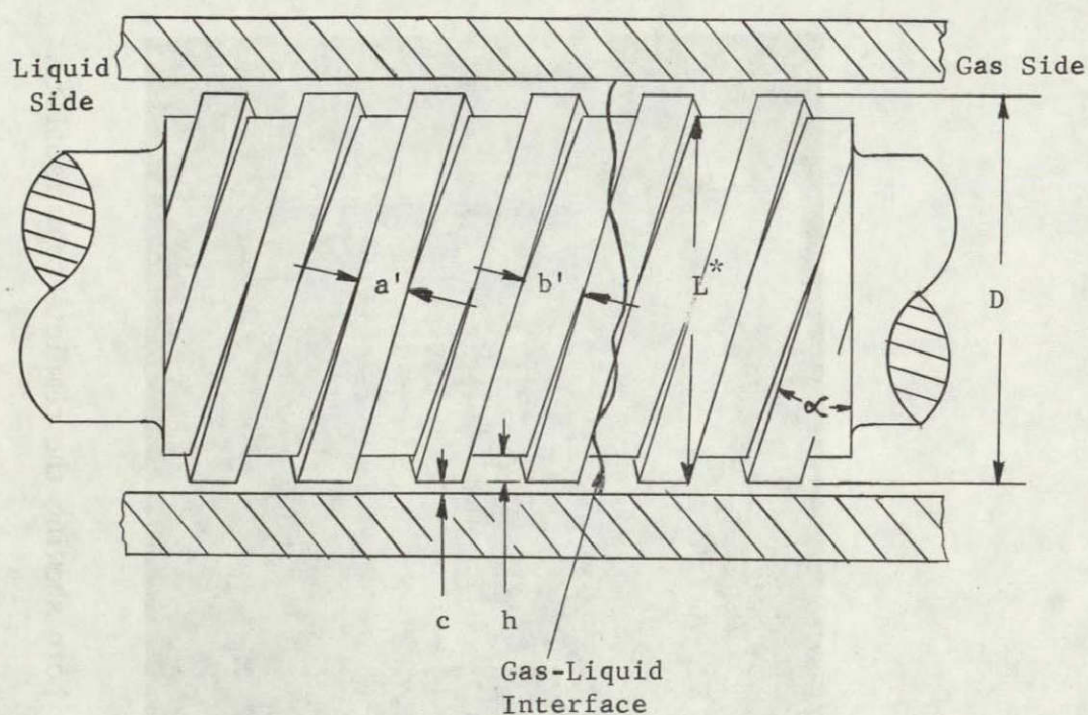


Figure 7. Illustration of viscoseal dimensions.

TABLE I
ROTOR DIMENSIONS

Seal	11	12	13	14	15
n	3	6	12	2	5
D	3.990	3.990	3.990	3.990	3.990
α	14.5	14.5	14.5	14.5	14.5
c	0.006	0.006	0.006	0.006	0.006
h	0.045	0.045	0.045	0.045	0.045
β	8.5	8.5	8.5	8.5	8.5
L^*	4.188	2.094	1.047	6.268	2.507
a'	0.524	0.262	0.131	1.045	0.104
b'	0.524	0.262	0.131	0.524	0.524
γ	0.5	0.5	0.5	0.334	0.834
b'/h	11.63	5.83	2.91	11.63	11.63

The transparent acrylic plastic housing was held in place by four long bolts connecting the base plate and a circular steel plate on top of the housing. The housing had an inside diameter of 4.002 inches which gave an average radial clearance of six mils. Eight pressure taps were located one inch apart in a line up and down the cylinder. Alignment of the housing and rotor was achieved by using paper feeler gages with a thickness of at least two mils. The minimum clearance in all tests was estimated to be no less than three mils.

The sealed cavity was located below the rotor with the annulus open to the atmosphere at the top. Fluid was introduced into the cavity and annulus through a hole in the base with a valve fitted into the passage to seal off the cavity. By filling the cavity and annulus from the bottom, it was possible to exclude any air bubbles from these regions.

No provision was made for cooling the sealing fluid although the temperature was measured with a 34 gage copper-constantan thermocouple inserted in an unused pressure tap. The pressure gradient was measured by connecting a mercury filled manometer to the fourth and sixth pressure taps from the top using flexible plastic tubing which was clear enough to be seen through and thus inspected for air bubbles. Speed was measured using a stroboscope, which also aided in visual observations.

Distilled water as well as silicone fluids of two, five, and ten centistoke viscosity were used as sealing fluids. The pertinent properties of these fluids are listed in Table II.

2. Inertial Test Procedures.

The inertial tests consisted of measuring the pressure and temperature generated by the seal at speeds from about 300 rpm to 3600 rpm. Speeds lower than 300 rpm were avoided since errors in pressure measurement tended to be significant at such low pressure magnitudes.

At high speeds the influence of gas ingestion and temperature rise required that only two to three sets of speed, temperature, and pressure data could be taken at a time. With an increase in

TABLE II
SEALING FLUID PROPERTIES

Fluid	Surface Tension (dyne/cm)	Specific Gravity	Viscosity (centistokes)
Water	72.8*	1.0	0.885
Silicone	18.7	0.873	2.0
Silicone	19.7	0.920	5.0
Silicone	20.1	0.940	10.0

* This value taken at 68°F

All values, except as noted, are for 77°F.

temperature, the physical dimensions of the rotor and housing changed as each expanded. This expansion gave a different radial clearance than that used in the computations. Tests showed that a 40° F rise in temperature (70° to 110° F) increased the diameter of the rotor by 0.003 inches and the inside diameter of the housing by 0.007 inches. Therefore, the data were taken in a range of temperatures from 70° F to 80° F. Data were taken before gas ingestion became severe, and the gas was cleared from the sealed cavity and annulus before new data were taken. In some cases this involved reaching the desired speed and obtaining data in one to two minutes. The pressure lines were also carefully checked for gas bubbles in them which would affect the pressure measurement.

3. Ingestion Test Apparatus.

The same test facility was used for the ingestion studies that was used for the inertia studies with some modification. In the backflow tests, a pressurized liquid-filled tank and flow measuring device were added. Fluid in the tank, pressurized by an inert gas, was delivered into the sealed cavity and annulus by way of the passage normally used to introduce fluid into the cavity before running the seal. The flow was measured using a Fischer-Porter Tri-Flat Variable-Area Flowmeter which measured flow up to 11 ml/sec. Only distilled water was used in this apparatus. Backflow fluid for long term tests was provided by connecting the building tap water supply to the flowmeter.

The centrifugal separator, Figure 2, page 6, essentially consists of an inner cavity connected with the groove surface by 12 radial flow passages, six at each of two levels, and connected with the atmosphere by two passages in the top of the seal. Seal 12, with six thread starts, was modified to form the separator and was designated seal 12-A. The lower passages were located to open into the grooves near the leading edge since almost all air bubbles are transported in this region. The opening into the grooves was also countersunk to more effectively catch the bubbles. The countersinks were later replaced by 1/16 inch deep, 1/4 inch diameter holes

and the seal designated 12-B. Since some of these holes did not fully extend to the ridge wall at the leading edge of the groove, they were extended to do so, and the seal was designated 12-C.

The centrifugal separator was designed to operate at 3600 rpm and 70° F. At these conditions, enough pressure should be generated at the lower passage level by the pumping action of the seal to overcome the pressure differential across the lower passages created by centrifugal acceleration. The pressure should also be high enough to support the pressure drop due to friction through the two sets of passages. Thus a flow loop is set up which carries air bubbles into the cavity where they are separated to the inside of the fluid layer on the cavity wall by centrifugal action. The air is allowed to escape to the atmosphere through the top holes, and the fluid returns to the annulus by way of the top passages. This flow loop is in contrast to Boon's recirculator which dumped the air back into the annulus and also circulated air only.

Several aspects of the operation of the separator which were considered in its design are worthy of mention here.

1. The upper flow passages must be flooded at all times to prevent air from being forced back into the annulus.
2. The lengths of the passages must be chosen so that the pressure change across the lower passages due to centrifugal acceleration can be overcome by the pressure generation due to the pumping action of the seal. Otherwise, there will be no flow through the passages.
3. The size of the passages will regulate the flow rate through them and determine the pressure drop through them due to friction. The sum of the pressure drops due to friction through the passages must be less than the pressure at the lower level generated by the pumping action of the seal. This condition will insure a flow through all passages.
4. The axial distances between the lower passages and the upper passages and between the lower passages and the top fluid level or interface must be chosen so as to provide enough

pressure at the lower levels due to pumping to overcome the pressure drops due to friction and centrifugal acceleration in the passages.

5. The flow rate of the flow loop must be large enough to sweep the air bubbles from the grooves. However, if it is too large, the pressure drop in the annulus between the two passage levels due to this flow will significantly affect the pressure generation of the seal.
6. The centrifugal separator will tend to regulate the fluid flow and seek some equilibrium operating conditions. At these conditions the flows through the upper and lower passages will be the same, and the net pressure at the outer opening of the upper passages will be equal to the pressure generated by the length of the seal from this point to the interface. This length is termed k . The two passage flows are related to k as shown in Figure 8.

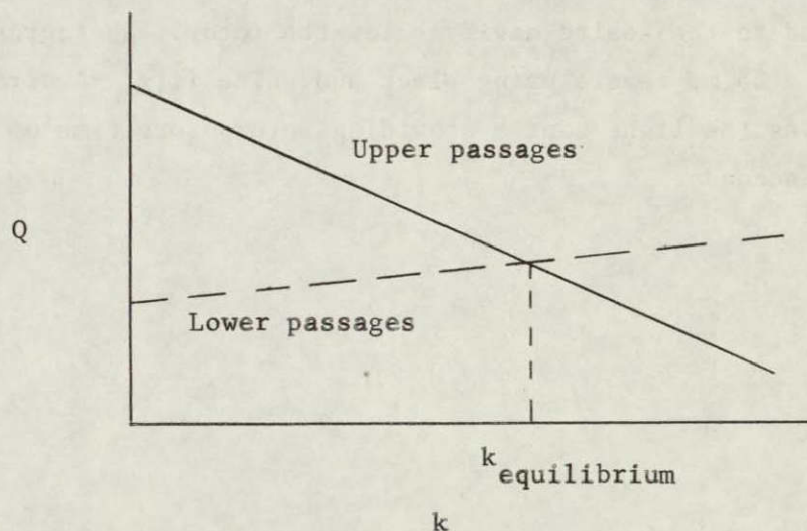


Figure 8. Passage Q versus k for the centrifugal separator.

If, for instance, the upper passage flow increases, then the amount of fluid in the annulus will increase. According to Figure 8, a high k will give a lower flow rate in the upper passages and a higher flow rate in the lower passages. Therefore, the amount of fluid in the annulus will decrease and k will decrease.

7. The velocity through the passages must be limited to prevent cavitation. This condition could occur in the top passages where the fluid enters at almost atmospheric pressure, and due to the vena contracta the pressure decreases further.

The final design of the centrifugal separator was reached through a trial and error process until all of the criteria mentioned above were met.

4. Ingestion Test Procedures.

In order to make comparisons among seals 12, 12-A, 12-B, and 12-C, tests were made with identical speeds, initial temperatures, interface levels, time intervals, and sealing fluids. Some tests were made at slowly increasing speeds to observe the onset of ingestion or the start of bubble capturing by the lower passages. Other tests were made at a constant speed for a given time.

The degrees of ingestion were compared by comparing the amount of air in the annulus and/or the amount of air which had been transported to the sealed cavity below the rotor. Photographs were made with a 35 mm camera using black and white film. A stroboscope was used as the light source providing an exposure time of about 1.2 microseconds.

CHAPTER IV

RESULTS AND CONCLUSIONS

1. Inertial Test Results.

The results of the inertial tests are shown in Figures 9 and 10 in the form of log-log plots of sealing coefficient versus Reynolds number. Also, Table III gives a comparison of transition Reynolds numbers as predicted by several different equations along with the actual experimental values.

Figure 9 shows the performance of seals 11, 14, and 15 which had identical values of α , β , and b'/h but varying values of L^* and γ . As can be seen, the experimental values of Δ agree reasonably well with the theory according to Stair and Hale (6), which does not directly include inertia effects or consider L^* as a parameter affecting seal performance. It is also noted that the transition points for the three seals are all relatively close, being in a range of Re_c values of 100 to 200. According to the prediction that the transition should take place at $Re^* = 1.0$, the Re_c values of transition should have been 697, 105, and 418 for seals 11, 14, and 15 respectively. The data does not agree with this prediction.

Figure 10 shows the experimental results for seals 11, 12, and 13 which had common values of α , β , and γ , but varying L^* and b'/h . According to the analyses of Stair and Hale (6), Pape and Vrakking (7), and Vohr and Chow (24), the theoretical performance of these three seals would be represented by a single curve for each analysis. As is seen, the experimental performance of the three seals is practically the same well into the turbulent regime. However, in the transition region the performance of each is distinctly different from the others. Since L^* and b'/h are the only variants, and Figure 9 shows L^* to have essentially no effect on performance, it is likely that the aspect ratio causes this difference. Furthermore, Zuk (1) suggested that as the aspect ratio increases, the breakpoint decreases, and he pointed out that data taken by Stair (25) showed this trend. Figure 10 also shows this trend in seals 11,

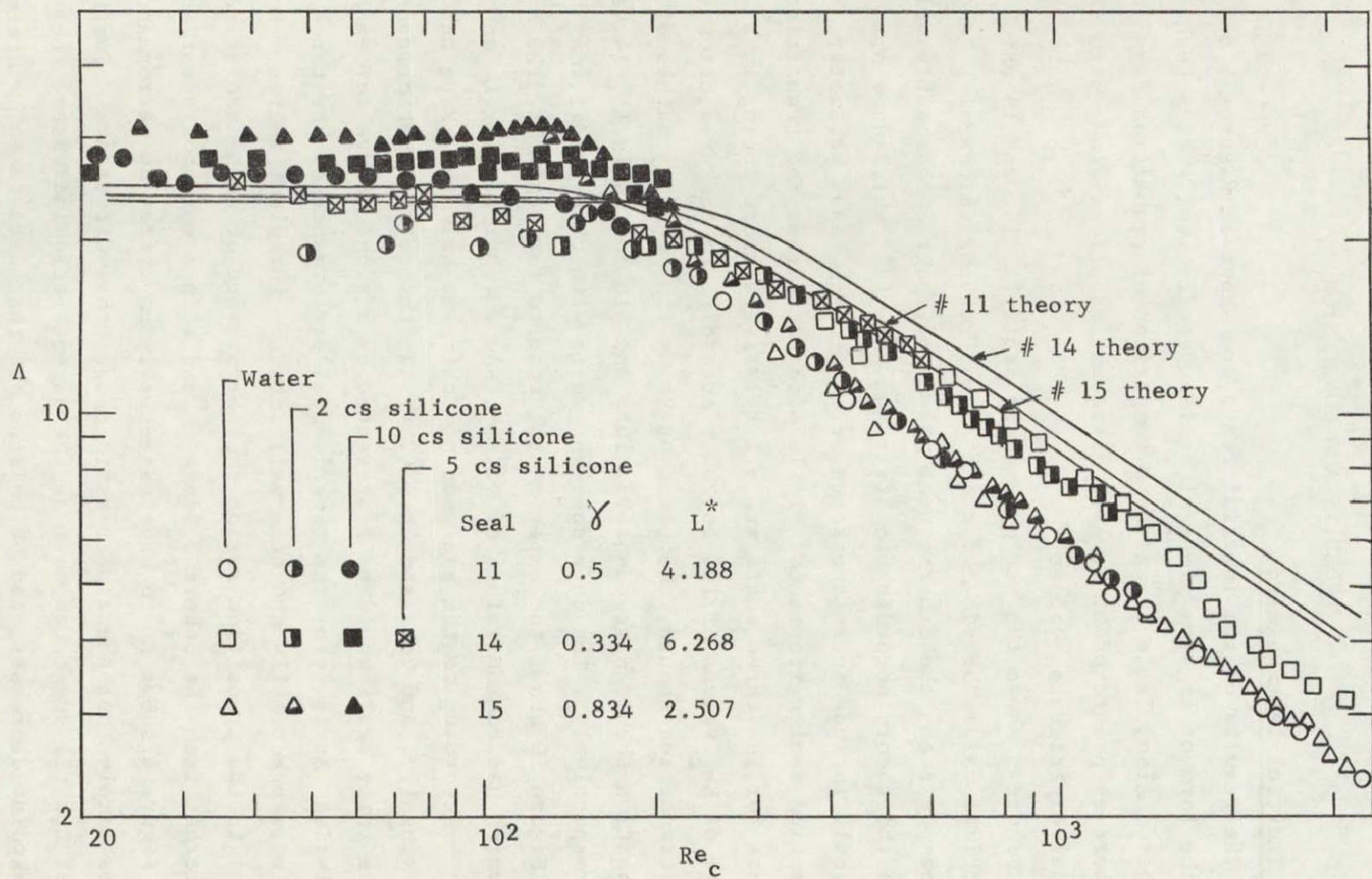


Figure 9. Experimental performance of seals 11, 14, 15.

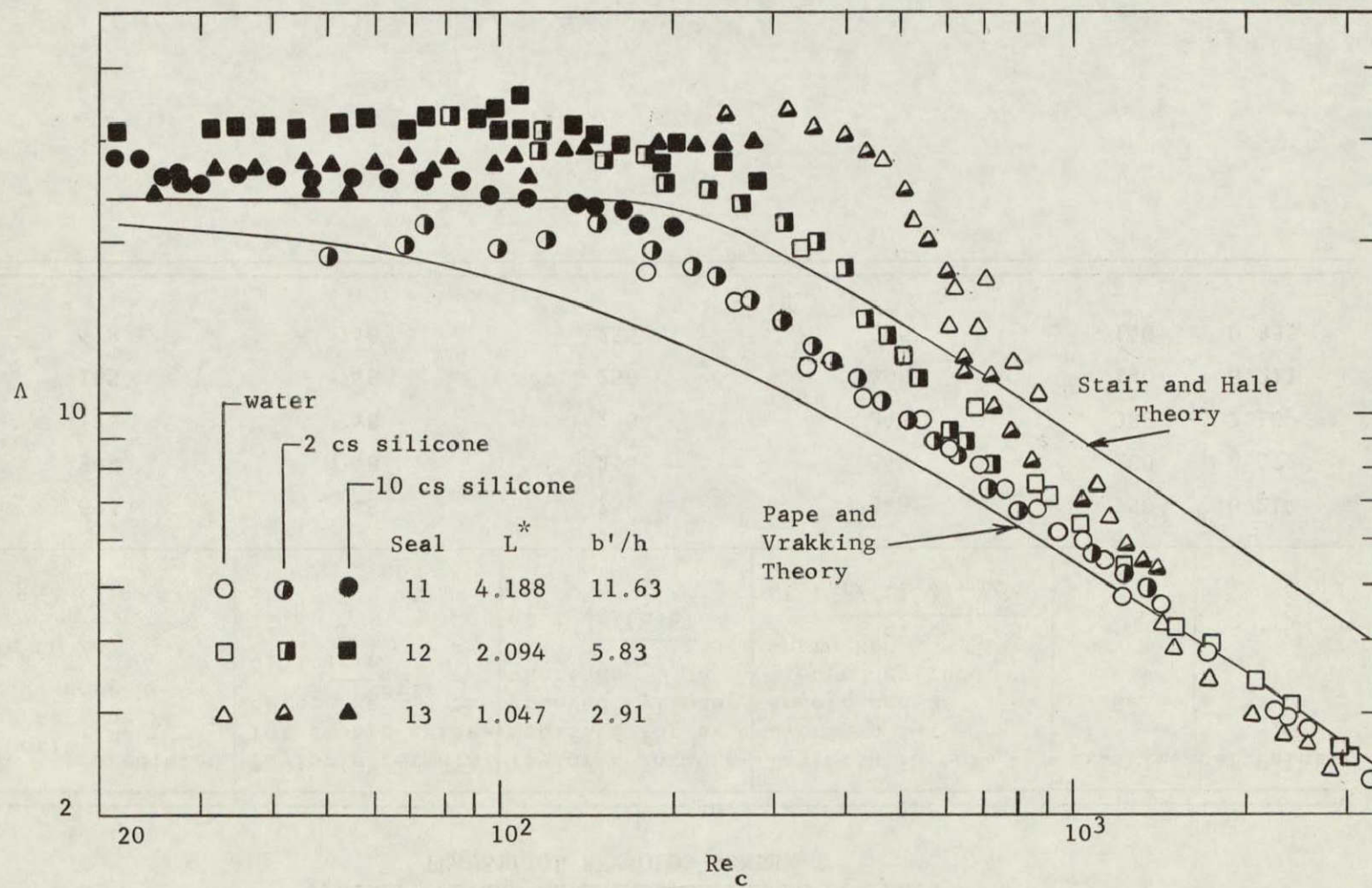


Figure 10. Experimental performance of seals 11, 12, 13.

TABLE III
THEORETICAL AND EXPERIMENTAL VALUES OF THE
TRANSITION REYNOLDS NUMBER

Seal	Re _{crit} predicted by setting Re* = 1.0 where Re _c = Re* (L*/c)	Taylor's formula for smooth cylin- ders: Re _{crit} ≤ 41.1 √r/c	Taylor's formula modified for a grooved cylinder where Re _{crit} ≤ 41.1 √r/(h+c)	Taylor's formula averaged for a smooth and a grooved cylinder where Re _{crit} ≤ 41.1 √r/((1-δ)+γβc)	Experimental Values	
					Re _c	Re*
11	697	748	256	343	150	0.214
12	349	748	256	343	200	0.572
13	175	748	256	343	380	2.18
14	105	748	256	400	190	0.211
15	418	748	256	285	140	0.335

12, and 13. Seals 11, 14, and 15 had equal aspect ratios, and their transition points are relatively close as mentioned previously.

It therefore appears that L^* has a negligible effect on seal performance and that the reduced Reynolds number based on L^* does not predict with precision the transition Reynolds number. The critical Reynolds number based on Taylor's criterion for the onset of turbulence in concentric, rotating cylinders, modified to include the effects of grooves on the inner cylinder, most accurately predicted the transition Reynolds number in four of the five seals. Furthermore, the effects of aspect ratio on performance appeared to be significant only in the transition region where a higher aspect ratio gave a lower value of the transition Reynolds number.

The gas ingestion in the five seals was observed and noted, although not studied in great detail. Each seal, except seal 15, ingested enough air at 3600 rpm in a certain period of time, which was different for each seal, to rather violently blow liquid from the annulus. Seal 13 with 12 thread starts had the highest ingestion rate and accumulated enough air under the rotor in two minutes at 3600 rpm to blow liquid from the annulus. The times for the same occurrence in the other seals are as follows: 15 min. for seal 11; 10 min. for seal 12; and 4 min. for seal 14. Seal 15 was not operated long enough to blow liquid from the annulus although it once was operated for thirty minutes with little gas accumulation. As is shown in Table I, page 19, it had very narrow lands and wide grooves which parallels evidence reported by Stair (2) that such a geometry resulted in reduced gas ingestion.

Operation with the silicone fluids resulted in much lower rates of ingestion for all seals. With the two centistoke fluid, small amounts of air reached the sealed cavity in seals 13 and 14 at high speeds, but no fluid was blown out. With the ten centistoke fluid, very little ingestion was noted for any of the seals. These results somewhat contradict the stability analysis of Fisher (9) which theoretically showed that fluids with higher viscosity and lower surface tension should result in more gas ingestion due to a more unstable interface.

2. Ingestion Test Results.

Testing of the centrifugal separator showed that it did capture air bubbles from the annulus at the bottom row of radial passages. Also, fluid could be observed flowing from the top passages by lowering the interface slightly below them. It did not appear that any bubbles were flowing with the fluid back into the annulus from these top passages, so the bubbles must have been separated out from the fluid while in the cavity as was predicted.

Before modification for centrifugal separation, seal 12 could accumulate enough air under the rotor in about ten minutes at 3600 rpm to blow most of the water up and out of the annulus, completely breaking down the sealing action. Ingestion appeared at the lowest speeds observed (200-300 rpm) and increased with increasing speed. In one test, the ingestion was observed by increasing the speed in steps beginning at 550 rpm and reaching 1910 rpm in about 50 minutes. The speed was then increased to 3680 rpm for six more minutes; and upon slowing the speed, the ingested air blew water from the annulus at about 3000 rpm. The speed was further decreased for about eight minutes down to 2300 rpm until there was no liquid in the annulus. The temperature reached 136° F before the slowing began. No tests were made for longer periods of time than this due to the lack of cooling and the subsequent high temperatures encountered.

An almost identical test was made with seal 12-A with centrifugal separation. The speed was increased in steps for about 45 minutes up to 3600 rpm and held there for 15 additional minutes. Upon slowing, no water was blown from the annulus, and only about 1-1/2 to 2 in.³ of air had accumulated under the rotor.

Seal 12-A ingested gas at the lowest speeds just as did seal 12. At about 800 rpm, bubbles coming from the interface began disappearing into the lower passages, and up to about 1200 rpm all ingested air was taken in at these passages. The size of ingested bubbles decreased somewhat with increasing speed, and at speeds above 1200 rpm, these small bubbles (roughly 0.04 inches in diameter) would slip under or by the countersinks along the leading edge of the grooves. This occurrence was particularly evident at some of the

countersinks which did fully extend to the leading edge of the groove. Beginning at approximately 2200 rpm, ingestion became great enough that large groups of bubbles would pass the lower passages along the full width of the groove. However, even at the highest speed of 3600 rpm, there was less ingested air below the bottom row of passages than above them as the passages captured part of the oncoming air.

To more effectively capture the ingested air bubbles, the countersinks were replaced by 1/16 inch deep, 1/4 inch diameter holes which extended nearly the full width of the grooves. There was a significant improvement in the ability of the lower passages to capture ingested air with these holes. The flow into the lower passages began at about the same speed as in 12-A, but bubbles still began passing the holes also at the same speed as in 12-A. However, the bubbles were reduced in size as they passed the holes to approximately 0.02 inches in diameter. Some holes were better than others at capturing the oncoming air, and upon close inspection, it was found that some of the holes did not fully extend to the leading edge of the groove, leaving about a 0.02 inch width of groove. These holes did not catch bubbles as effectively as those which actually touched the ridge wall at the groove leading edge. Therefore, these holes were extended to the groove edge and the seal designated 12-C. Figure 2, page 6, shows a hole as modified for seal 12-C.

Again, an improvement in the ability to capture ingested air was noted for seal 12-C, although 12-C also allowed ingested air to reach the sealed cavity. At speeds between 1200 rpm and 2200 rpm, only very tiny bubbles passed the holes along the groove leading edge. As in 12-A and 12-B, the ingestion became great enough at speeds over 2200 rpm that groups of bubbles passed the holes along the full width of the groove.

Figures 11, 12, and 13 show the progressive increase of the ingestion. Figure 11, at $Re_c = 770$ (900 rpm) shows fairly severe ingestion in water above the lower level of holes but none below the holes. Figure 12, at $Re_c = 1560$ (1800 rpm), shows some bubbles

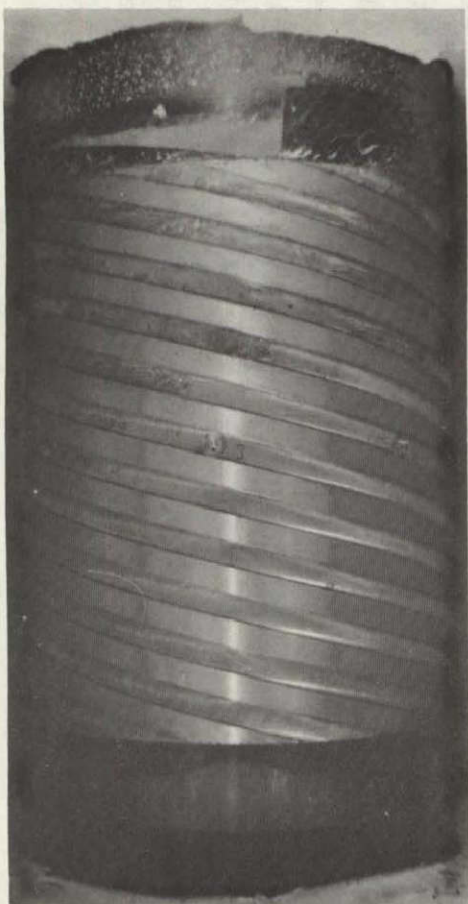


Figure 11. Seal 12-C at $Re_C = 770$ (900 rpm), $T = 71^\circ \text{ F}$, operating with water.

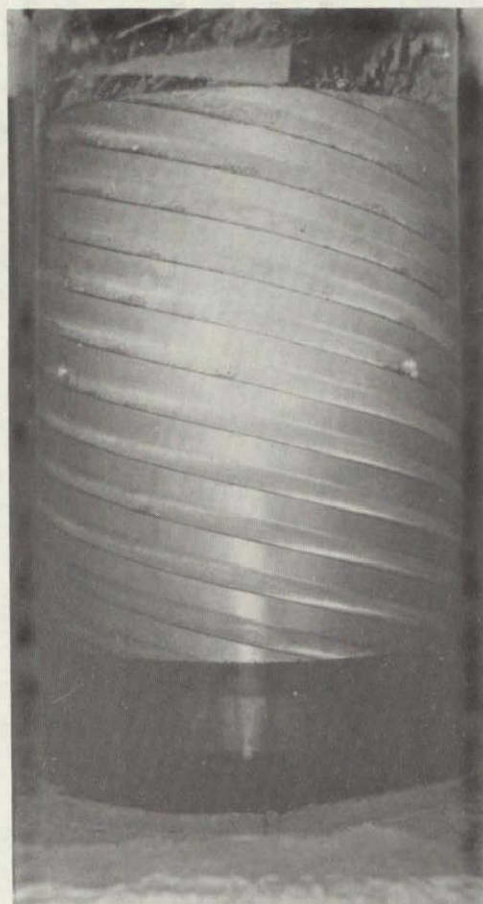


Figure 12. Seal 12-C at $Re_C = 1560$ (1800 rpm), $T = 72^\circ \text{ F}$, operating with water.



Figure 13. Seal 12-C at $Re_C = 2000$ (2200 rpm), $T = 82^\circ \text{ F}$, operating with water.

below the lower level of holes and also shows how the small bubbles collect into larger packets of bubbles both above and below the lower level of holes. Figure 13, at $Re_c = 2000$ (2200 rpm), shows a larger amount of air in the form of large packets below the lower level of holes. These packets pass the holes nearly the full width of a groove.

A larger amount of the ingested air was captured by the holes in 12-C than in both 12-A and 12-B, particularly at speeds up to 1600 rpm and over 3500 rpm. In a ten minute test at 1200 rpm, 12-A accumulated $1\frac{1}{2}$ in.³ of air under the rotor, 12-B accumulated $\frac{1}{4}$ in.³ of air, and 12-C accumulated only a few small bubbles. The same results were found in a ten minute test with the speed slowly increased from 400 rpm to 1200 rpm. In a 30 minute test, primarily at speeds of 2000 rpm to 3600 rpm, 12-A accumulated about 3 in.³ of air, 12-B accumulated $2\frac{1}{2}$ in.³ of air, and 12-C accumulated $1\frac{1}{2}$ in.³ of air. At speeds between 1600 rpm and 3500 rpm seals 12-B and 12-C were about the same in ingesting air, both showing improvement over 12-A of about 30%.

The most significant results were found at the design speed of 3600 rpm. As mentioned before, seal 12 would operate at 3600 rpm for only about ten minutes before the quantity of accumulated air became great enough to force liquid from the annulus. Seal 12-C was operated for one hour at 3600 rpm with the temperature reaching 150° F. No fluid was blown out, and about $2\frac{1}{2}$ in.³ of air was accumulated under the rotor. Furthermore, a major part of this air was accumulated in the first 15 minutes of operation. A major increase in temperature also took place in the first 15 minutes of operation after which the increase began to taper off. Figure 14 shows how both accumulated air and temperature increased with time. The seal tended to approach some equilibrium operating condition at which air was still ingested and appeared along the full length of the rotor, but it was not pumped under the rotor. There was a small loss of liquid from the annulus and a slight drop in interface level likely due to the liquid being sloshed out the top of the housing-rotor assembly and due to some evaporation of liquid at the high temperatures.

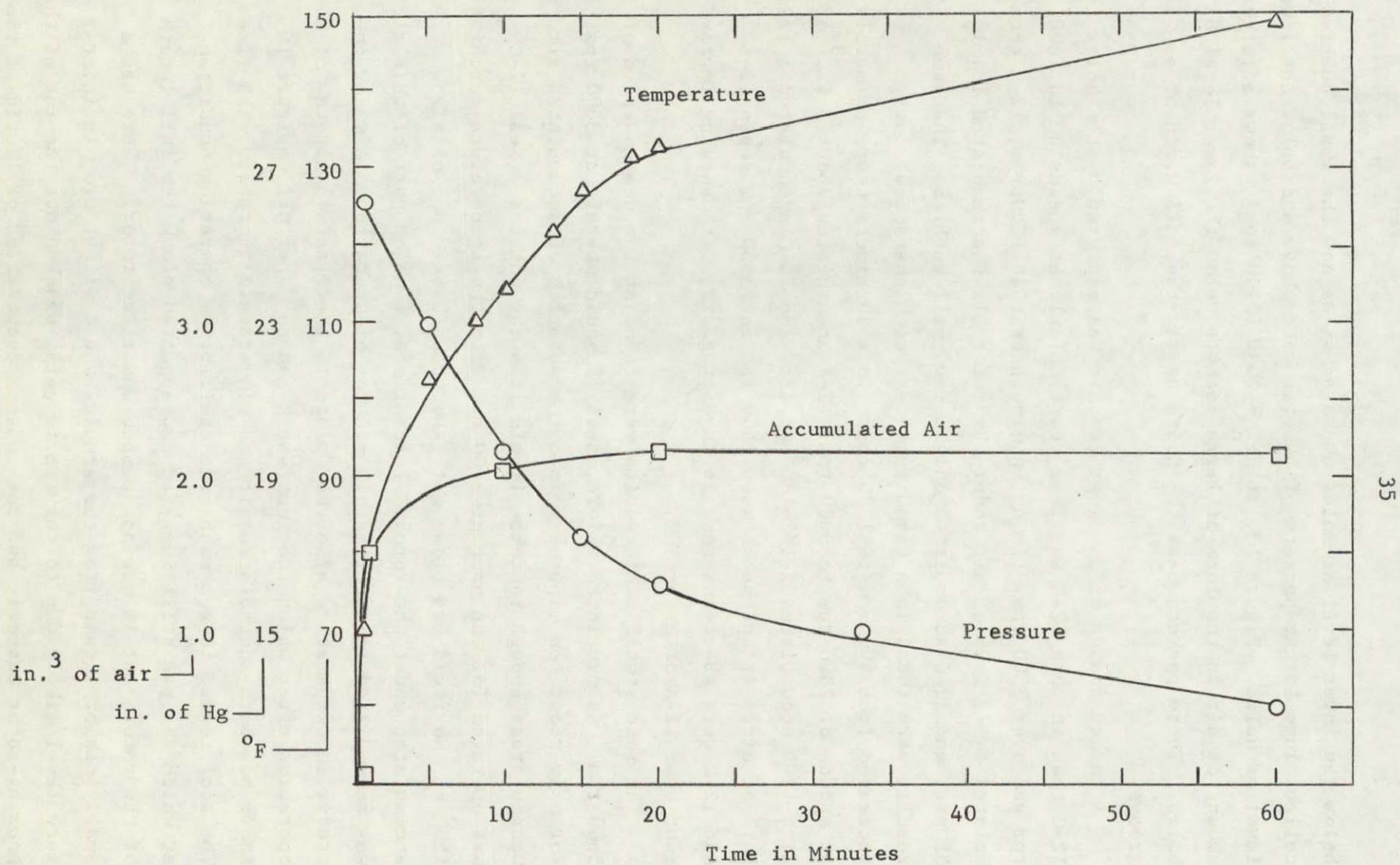


Figure 14. Temperature, pressure, and accumulated air versus time in seal 12-C at 3600 rpm.

The effect of temperature on ingestion was significant as several tests at lower temperatures produced a decrease in accumulated air. Tests were made at identical speeds for the same periods of time but with a ten degree decrease in initial temperature (70°F to 60°F). A 90% decrease in air accumulated below the rotor was noted at 1600 rpm, with an 85% decrease at 2000 rpm, 80% at 2600 rpm, and 50% at 3400 rpm. Also, at all speeds used in testing seal 12-C, no air passed the lower row of passages in the first one to two minutes of operation when the temperature had risen only a few degrees at most.

Figures 15 to 18 show the increase in ingestion with increasing time and temperature at 3600 rpm. Figure 15 was taken within one minute after the speed was reached at 71°F with fairly severe ingestion above the lower holes but none below. Figures 16, 17, and 18 were taken at 5, 10, and 15 minutes at temperatures of 95°F , 112°F , and 125°F respectively. There is not a very big difference in the degree of gas ingestion among Figures 16, 17, and 18, and there is little change in even longer periods of time. However, all show a significant increase over Figure 15 in the amount of air below the lower holes. Figure 19 shows the gas ingestion in seal 12 before modification at 3600 rpm after one to two minutes of operation. Figure 15 shows quite an improvement in ingestion at almost identical conditions.

The temperature may have affected ingestion by controlling the viscosity of the fluid. Lower temperatures yield higher viscosities, and the ingestion was less severe when the high viscosity silicone fluids were used in all of the seals tested. In testing seal 12-C with the two centistoke silicone, the ingested air did not begin to pass the lower passages at 3600 rpm until a temperature of 123°F was reached after running for about eight minutes. After a total run time of ten minutes and a temperature of 130°F was reached, only a small bubble of air had accumulated below the rotor. In running 12-C with the ten centistoke silicone, a few tiny bubbles began passing the lower passages at 132°F after ten minutes at 3600 rpm. No air reached the bottom of the rotor.

A temperature increase also decreases the surface tension of the fluid which could have contributed to the increased ingestion rates



Figure 15. Seal 12-C within one minute of the beginning of operation at 3600 rpm, $T = 71^{\circ}$ F, operating with water.



Figure 16. Seal 12-C at 3600 rpm, $t = 5$ min., $T = 95^{\circ}$ F, operating with water.



Figure 17. Seal 12-C at 3600 rpm, $t = 10$ min., $T = 112^{\circ}$ F, operating with water.



Figure 18. Seal 12-C at 3600 rpm,
 $t = 15$ min., $T = 125^{\circ}$ F, oper-
 ating with water.

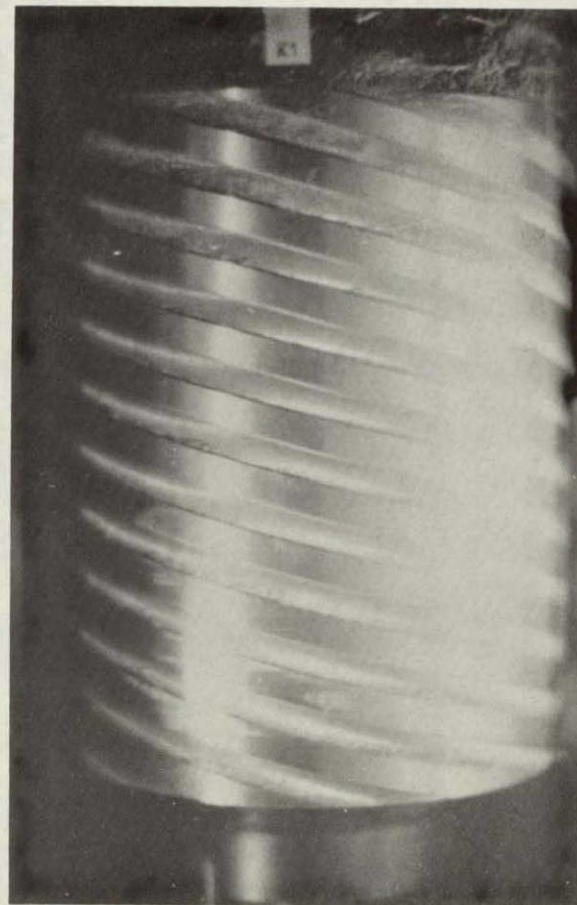


Figure 19. Seal 12 within one to two
 minutes of the beginning of ope-
 ration at 3600 rpm, $T = 75^{\circ}$ F,
 operating with water.

at high temperatures. Fisher's stability analysis (9) predicted increased ingestion at lower values of surface tension. His analysis also predicted increased ingestion at higher viscosities which was not the case with the silicone fluids in all seals tested for this study. The silicones also had a much lower surface tension than water which should have produced higher ingestion rates according to Fisher's analysis and also according to the results of the water tests. This result shows a contradiction in effects of surface tension on ingestion. Therefore, it appears that the effect of temperature on viscosity and the effect of viscosity on ingestion are more significant than that of surface tension.

The effect of temperature on the solubility of air in water and the relation between solubility and gas ingestion was also considered. It is possible that some ingestion results from air coming out of solution with water since the air is less soluble at higher temperatures. However, air is more soluble with increasing pressure. A mathematical estimation of the amount of air which could result from insolubility at the pressures and temperatures which were encountered in the viscoseal tests revealed that it was negligible.

It is estimated that the rate of gas accumulation in the sealed cavity was reduced by an order of magnitude in seal 12-A and was further reduced by about 30% to 40% in seal 12-C. While the exact explanation was not determined for the failure of 12-C to completely eliminate ingestion in the lower half of the seal, it is likely due to the fact that the magnitude of the flow through the passages was not large enough to sweep all of the oncoming air. Since the temperature rise and the presence of ingestion in the upper half of the annulus both reduce the pressure generated by this portion of the seal, it is probable that the reduction in pressure significantly reduced the magnitude of flow into the cavity. Figure 14, page 35, shows the reduction in Δp with time measured in seal 12-C at 3600 rpm. This explanation is somewhat illustrated by the fact that all of the ingested air was taken in by the lower passages in the first one to two minutes of operation of the seal before the temperature rose significantly and the ingestion became severe in the top half

of the annulus. Also, the holes captured air bubbles more effectively in the silicone fluids which generated a higher $\Delta p / \Delta L$ than water for a given speed and also caused less severe ingestion in the top half of the annulus.

Figures 20 and 21 show the sealing performance of seals 12-A and 12-C as compared to the unmodified seal. The figures show that the circulating flow loop had a negligible effect on the sealing performance. As mentioned previously, this data was taken with little air ingestion present or little temperature increase.

3 Backflow Test Results

Backflow tests on seals 11, 12, and 13 showed that a flow in the direction opposite to that of the pumping action of the seal does sweep out air ingestion. Tests also showed that merely having a small net flow in this direction did not sweep out all of the existing ingestion and prevent ingestion from proceeding back down to the high pressure end of the seal. Instead, the flow had to be of a certain magnitude that was dependent upon the seal geometry, the rotor speed, and the temperature of the backflow fluid and the fluid in the annulus.

In seal 11, the maximum flow of 11 ml/sec would sweep out roughly half of the existing ingestion in the annulus at all speeds tested. However, only at speeds up to about 1500 rpm would this flow prevent ingestion from slowly proceeding back down to the bottom of the rotor. As the valve was opened and the flow introduced into the sealed cavity, a surge of fluid into the annulus occurred, possibly due to pressure build-up in the flexible lines carrying the flow to the valve. At speeds above 1500 rpm, this surge of fluid temporarily swept the ingestion upward, and, after a steady backflow was reached, the ingestion was transported back toward the bottom of the rotor. The temperature of the flow was important as was shown in a test at 2500 rpm with a flow of 6 ml/sec provided by the building's water system. After running for 15 minutes and reaching 82° F with ingestion reaching down to the bottom of the rotor, the temperature began to decrease due to cooler backflow water flowing into the annulus. The temperature dropped several

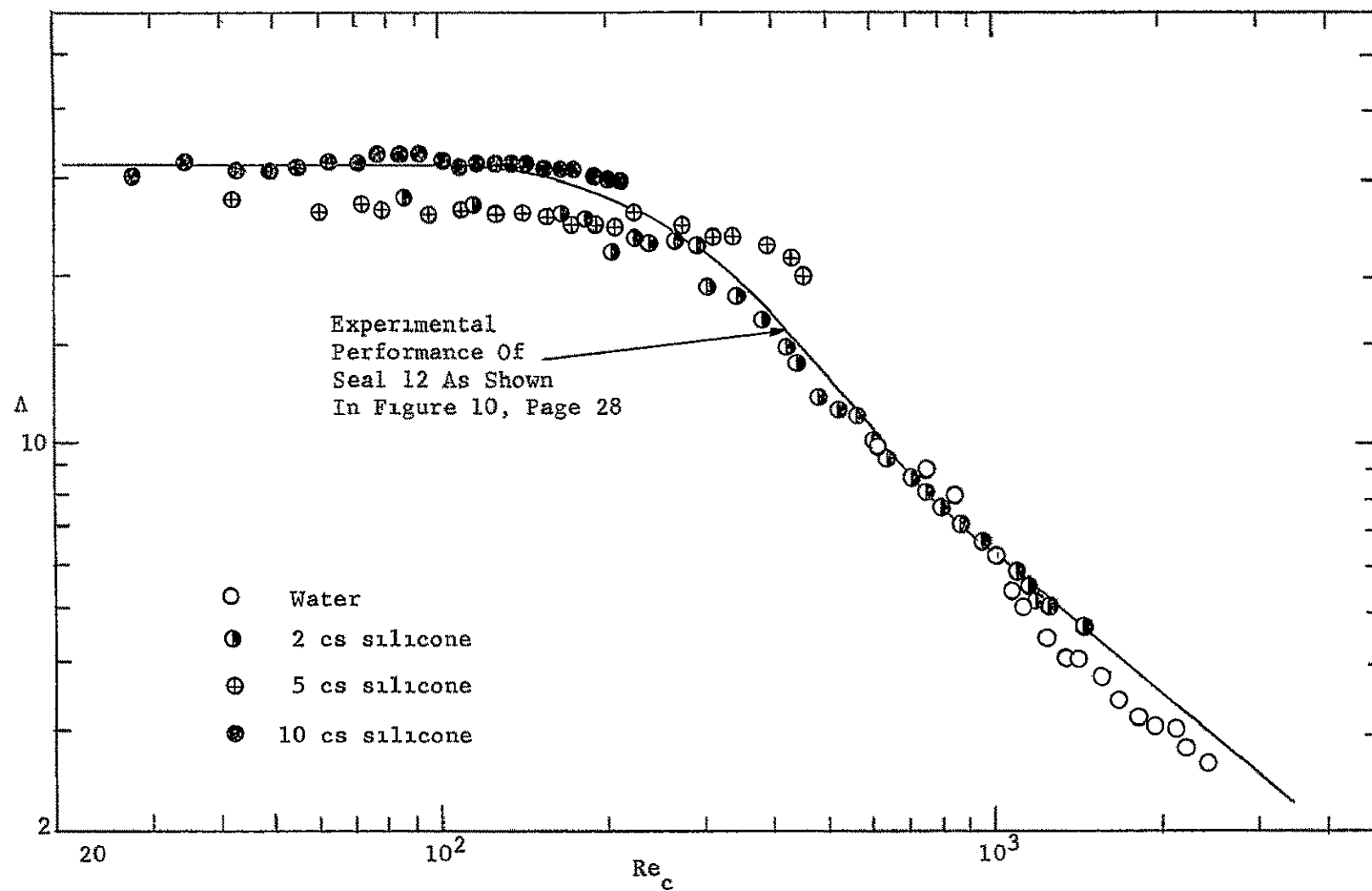


Figure 20 Experimental performance of seal 12-A

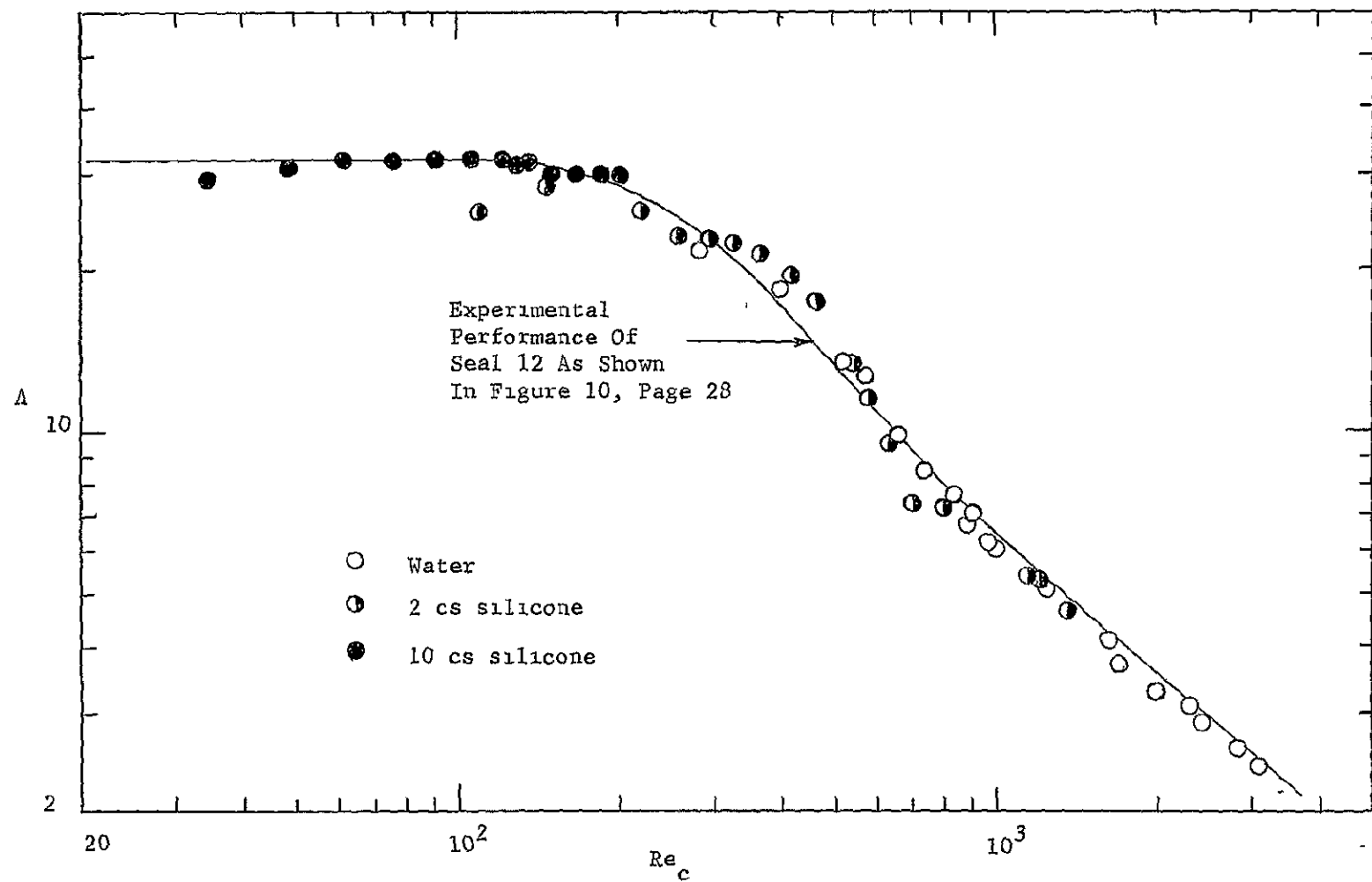


Figure 21 Experimental performance of seal 12-C

degrees, and there was a significant decrease in the amount of air ingestion in the annulus

The magnitude of flow necessary to prevent transport of ingested gas to the bottom of the rotor increased with increasing rotor speed and temperature which means it increased with increasing rates of gas ingestion. This flow magnitude also increased for seal 12 and further increased for seal 13 as the ingestion rates also increased for these two seals. The initial flow also did not sweep out as much existing ingestion when initially turned on as in seal 11. Only about 1/3 of the ingestion was swept out in seal 13 and between 1/2 and 1/3 for seal 12. The 11 ml/sec flow would completely prevent the transport of ingestion in seal 12 at speeds up to 1200 rpm and at speeds up to 700 rpm in seal 13 in the temperature range of 70° F to 80° F.

The backflow affected the sealing performance by increasing the pressure gradient as read by the manometer. In seal 11, the 11 ml/sec flow increased the pressure gradient about 0.1 psi/in at all speeds. The increase was 0.13 psi/in for seal 12, and 0.15 psi/in for seal 13. At low speeds and subsequent low pressures, this increase reduced the sealing coefficient as much as 50% while the effect at high speeds and high pressures was negligible.

4 Conclusions

The major conclusions reached from this study are as follows

- 1 The characteristic length had negligible effect on sealing performance. The use of the modified Reynolds number based on characteristic length to predict the transition Reynolds number was not a precise way of predicting transition.
- 2 The aspect ratio affected sealing performance in the transition region where a higher aspect ratio gave a lower transition Reynolds number.
- 3 The centrifugal separator as existed in seal 12-A reduced the rate of gas accumulation in the sealed cavity by an order of magnitude. A further reduction was accomplished by providing larger and deeper catch holes at the entrance to the lower row of radial passages.

- 4 In long term operation, the centrifugal separator approached equilibrium operating conditions at which very little additional air was accumulated in the sealed cavity. The centrifugal separator therefore shows promise as an effective way to control gas ingestion in viscoseal operation without significantly affecting the sealing performance.
- 5 A backflow of fluid of suitable magnitude from the high pressure to the low pressure end of the viscoseal effectively swept out ingested gas and prevented transport of gas to the high pressure end of the seal.

BIBLIOGRAPHY

BIBLIOGRAPHY

- 1 Zuk, J , Ludwig, L P , and Johnson, R L , "Flow and Pressure Field Analysis of Parallel Groove Geometry for an Incompressible Fluid with Convective Inertia Effects," NASA TN D-3635, NASA, Washington, D C , September, 1966
- 2 Stair, W K , "Theoretical and Experimental Studies of Visco-Type Shaft Seals," Mechanical and Aerospace Engineering Research Report ME 64-587-1, University of Tennessee, October 23, 1964
- 3 Boon, E F and Tal, S E , "Hydrodynamische Dichtung for rotierende Wellen," Chemie-Ing-Technik, 31, 202-212, January 31, 1959
- 4 Asanuma, T , "Studies on the Sealing Action of Viscous Fluids," "International Conference on Fluid Sealing," Paper A3, B H R A , Harlow, Essex, England
- 5 McGrew, J. M and McHugh, J D , "Analysis and Test of the Screw Seal in Laminar and Turbulent Operation," The General Electric Advanced Technology Laboratories, Report No 63GL66, May 3, 1963
- 6 Stair, W K and Hale, R H , "Analysis of the Visco Seal, Part II, The Concentric Turbulent Case," Mechanical and Aerospace Engineering Report ME 66-587-7, University of Tennessee, June 28, 1966
- 7 Pape, J G and Vrakking, W J , "Viscoseal Pressure Generation and Friction Loss Under Turbulent Conditions, " ASLE Transaction 11, 4, 1968
- 8 King, A E , "Engineering Information Report on Tests Made with a Hydrodynamic Screw Seal (Viscoseal) in Oil, Water, and Potassium," Westinghouse Electric Corporation, Aerospace Electrical Division, Report No WAED 63 3 (Revision A), September, 1964
- 9 Fisher, C F., "An Investigation of Interface Stability and Its Relation to Gas Ingestion in Viscoseals," Doctoral Dissertation, University of Tennessee, August, 1969
- 10 Boon, R J G , "Observations on a Viscoseal in a Transparent Housing, The Prevention of Leakage and Breakdown," Master's Thesis, Technische Hogeschool, Delft, The Netherlands, June, 1968 Translated by Fluid Sealing Research Laboratory, University of Tennessee, Report ME 69-T57-4, March, 1969
- 11 Stair, W K , "Analysis of the Visco Seal, Part I, The Concentric Laminar Case," Mechanical and Aerospace Engineering Research Report ME 65-587-2, University of Tennessee, January 18, 1965
- 12 Schlichting, H , Boundary Layer Theory, McGraw Hill, 1965

- 13 Kettleborough, C F , "Turbulent and Inertia Flow in Slider Bearings," ASLE Transaction, Vol 8, No 3, July, 1965
- 14 Ketola, H N and McGrew, J M , "Turbulent Operation of the Viscoseal," ASLE Transaction 10, 1967
- 15 Rowell, H S. and Finlayson, D , "Screw Viscosity Pumps," Engineering, Vol 114, November 17, 1922, Vol 126, August 31, 1928, September 28, 1968
- 16 Weinand, L H , and Wroblewski, R.C , "The Principles of Hydrodynamic Sealing," Proceedings of Seal Symposium, September 30, 1965, General Motors Corporation Research Publication GMR-532
- 17 Golubiev, A I , "Studies on Seals for Rotating Shafts of High Pressure Pumps," Wear, Vol 8, No 4, July/August 1965
- 18 Holan, K , "Sealing in Engineering," Proceedings of the Second International Conference on Fluid Sealing, BHRA, Harlow, Essex, England, 1964
- 19 Frossel, W , "Untersuchung von Gewindewellendichtungen," Konstruktion, 18 Heft 4, 1966
- 20 D van der Meulen, "Onderzoek aan ien visco-ofdichting," 5e jaars rapport nr 2-67, Laboratory for Chemical Equipment, University of Delft, 1967.
- 21 Ludwig, L P , Strom, T N , and Allen, G P , "Gas Ingestion and Sealing Capacity of Helical Groove Fluid Film Seal (Viscoseal) Using Sodium and Water as Sealed Fluids," NASA TN D-3348, NASA, Washington, D C , March, 1966
- 22 Stair, W.K , "Theoretical and Experimental Studies of Visco-Type Shaft Seals," Mechanical and Aerospace Engineering Research Report ME 650587-4, University of Tennessee, October 20, 1965
- 23 Zuk, Strom, Ludwig, and Johnson, "Convective Inertia and Gas Ingestion Effects on Flow Regimes of the Viscoseal - Theory and Experiment, NASA TM X52283, NASA, Washington, D C
- 24 Vohr, J and Chow, C , "Theoretical Analysis of Spiral-grooved Screw Seal for Turbulent Operation," A paper presented at the Fourth International Conference on Fluid Sealing, Philadelphia, Pennsylvania, May, 1969
- 25 Stair, W K , "Theoretical and Experimental Studies of Visco-Type Shaft Seals," Mechanical and Aerospace Engineering Research Report ME 66-587-5, University of Tennessee, April 28, 1966

VITA

Lawrence Howard Luttrull [REDACTED]

[REDACTED] He attended elementary schools in that city and was graduated from Isaac Litton High School in June, 1964. The following September he entered the University of Tennessee and in June, 1968, he received a Bachelor of Science degree in Aerospace Engineering. He was also commissioned a Second Lieutenant in the United States Air Force. In the summer of 1968, he accepted a research assistantship at the University of Tennessee and began study toward a Master's degree. He is a member of Pi Tau Sigma and Tau Beta Pi national honoraries. Upon graduation he will enter into active duty with the Air Force.

He is married to the former Elizabeth Ann Watkins of Nashville, and they have a son Andrew Todd.

DISTRIBUTION LIST

Defense Documentation Center
Cameron Station
Alexandria, Virginia 22314

Mr P H Broussard
NASA, R-ASTR-GC
Marshall Space Flight Center
Huntsville, Alabama 35812

Mr John J Gurtowski
Naval Air Systems Command
Code AIR 52032C - Dept of the Navy
Washington, D C 20360

Mr Robert L Johnson
Chief, Lubrication Research Branch
NASA, Lewis Research Center
Cleveland, Ohio 44135

Mr W C Karl
Office of Naval Research, Code 473
Department of the Navy
Washington, D C 20360

Mr Lawrence P Ludwig
Head, Seals Section
NASA, Lewis Research Center
Cleveland, Ohio 44135

Mr Joseph Maltz
Materials Research Program
National Aeronautics & Space Adm
Washington, D C 20546

Col W Metscher
Office of Director of Defense Research
and Engineering
Room 3C128, Pentagon
Washington, D C 20301

Mr E R Taylor
Reactor Engineering Division
Oak Ridge National Laboratory
Oak Ridge, Tennessee 37830

Mr Marshall J Armstrong, Jr
U S Army Mobility Equipment Research
and Development Center
Fort Belvoir, Virginia 22060

Mr Richard N Belt
U S Army Mobility Equipment Research
and Development Center
Fort Belvoir, Virginia 22060

Mr Floyd Lux
U S Tank Automotive Center
Propulsion Systems Laboratory, SMOTA-RCP 4
Warren, Michigan 48090

Mr J R Crowder
Flight Mechanics & Fluid Systems Section
(AIR 5303)
Naval Air Systems Command - Dept of the Navy
Washington, D C 20360

Mr Roy R Peterson
Naval Ship Systems Command (Code 03413)
Department of the Navy
Washington, D C 20360

Dr Earl Quandt
Naval Ship Research & Development Center
Annapolis Division
Annapolis, Maryland 21402

Mr Alan Schrader
Naval Ship Research & Development Center
Annapolis Division
Annapolis, Maryland 21402

Mr Lyman Carlyle Fisher
Naval Ordnance Laboratory
Department F (Code 510) - White Oak
Silver Spring, Maryland 20910

Mr Stanley Doroff
Office of Naval Research (Code 438)
Department of the Navy
Washington, D C 20360

Mr John W Zmurk
Air Force Aero Propulsion Laboratory (APIP-1)
Wright-Patterson Air Force Base, Ohio 45433

Capt Kenneth R Hooks
Air Force Weapons Laboratory WLDC
Kirtland Air Force Base, New Mexico 87117

Dr Joseph F Masl
Air Force Office of Scientific Research, SREP
1400 Wilson Boulevard
Arlington, Virginia 22209

Mr Frank J Mollura
Rome Air Development Center, EMEAM
Griffiss Air Force Base, New York 13440

Mr Gerald S Leighton
SEPO - Division of Space Nuclear Systems
U S Atomic Energy Commission
Washington, D C 20545

Mr C E Miller, Jr
Division Reactor Development & Technology
U S Atomic Energy Commission
Washington, D C 20545

Bureau of Naval Personnel
Department of the Navy
Washington, D C 20370
Attn Technical Library

Naval Air Systems Command
Department of the Navy
Washington, D C 20360
Attn Technical Library Division, AIR-604

Naval Applied Science Laboratory
Flushing and Washington Avenues
Brooklyn, New York 11251
Attn Technical Library, Code 222

U S Naval Oceanographic Office
Suitland, Maryland 20390
Attn Library, Code 1640

U S Naval Postgraduate School
Monterey, California 93940
Attn Library, Code 0212

DISTRIBUTION LIST (Cont'd)

Naval Ship Engineering Center
Philadelphia Division
Philadelphia, Pennsylvania 19112
Attn Technical Library

Naval Ship Research & Development Center
Annapolis Division
Annapolis, Maryland 21402
Attn Library, Code A214

Naval Ship Systems Command
Room 1532 Main Navy
Washington, D C 20360
Attn Technical Library

U S Atomic Energy Commission
Argonne National Laboratory
9700 South Cass Avenue
Argonne, Illinois 60440
Attn Library

National Bureau of Standards
Washington, D C 20025
Attn Library

Battelle Memorial Institute
505 King Avenue
Columbus, Ohio 43201
Attn Library

Massachusetts Institute of Technology
Cambridge, Massachusetts 02139
Attn Library

Naval Undersea Warfare Center
3202 East Foothill Boulevard
Pasadena, California 91107
Attn Technical Library

Navy Underwater Sound Laboratory
Fort Trumbull
New London, Connecticut 06320
Attn Technical Library

U S Naval Weapons Laboratory
Dahlgren, Virginia 22448
Attn Technical Library

The Franklin Institute
Benjamin Franklin Parkway at 20th Street
Philadelphia, Pennsylvania 19103
Attn Library

Power Information Center
University City Science Institute
3401 Market Street, Room 2107
Philadelphia, Pennsylvania 19104

Aerojet-General Corporation
Von Karman Center
Azusa, California 91702
Attn Library

Aerojet-General Nucleonics
San Ramon, California 94583
Attn Library

University of Arizona
Department of Aerospace and
Mechanical Engineering
Tucson, Arizona 85721
Attn Professor Kececioğlu

AiResearch Manufacturing Company
9851 Sepulveda Boulevard
Los Angeles, California 90045
Attn Library

AiResearch Manufacturing Company
402 South 36th Street
Phoenix, Arizona 85034
Attn Library

General Electric Company
Flight Propulsion Division
Cincinnati, Ohio 45215
Attn Library

General Electric Company
Mechanical Technology Laboratory
Research and Development Center
Schenectady, New York 12301
Attn Library

DOCUMENT CONTROL DATA - R & D

(Security classification of title body of abstract and indexing annotation must be entered when the overall report is classified)

1 ORIGINATING ACTIVITY (Corporate author) University of Tennessee Knoxville, Tennessee Mech & Aero Engr Dept		2a REPORT SECURITY CLASSIFICATION Unclassified	
		2b GROUP --	
3 REPORT TITLE A Study of Convective Inertia Effects and Methods of Controlling Gas Ingestion in Large Diameter Viscoseals			
4 DESCRIPTIVE NOTES (Type of report and inclusive dates) Interim - March 1970			
5 AUTHOR(S) (First name middle initial last name) Lawrence Howard Luttrull			
6 REPORT DATE March 1970		7a TOTAL NO OF PAGES 48	7b NO OF REFS 25
8a CONTRACT OR GRANT NO NGR-43-001-003 and N00014-68-A-0144		9a ORIGINATOR'S REPORT NUMBER(S) ME 70-T57-10	
b PROJECT NO		9b OTHER REPORT NO(S) (Any other numbers that may be assigned this report) --	
c			
d			
10 DISTRIBUTION STATEMENT This document has been approved for public release and sale, its distribution is unlimited			
11 SUPPLEMENTARY NOTES --		12 SPONSORING MILITARY ACTIVITY --	
13 ABSTRACT <p>This study is concerned with the effect of two parameters, characteristic length and aspect ratio, on the performance of large diameter viscoseals, and with methods of preventing or controlling gas ingestion in viscoseals</p> <p>The characteristic length, or length of the groove-land pair in the direction of seal rotation, and the aspect ratio, or ratio of groove width to groove depth, arose as parameters likely affecting viscoseal performance in an analysis by Zuk, Ludwig, and Johnson, who included the convective inertia terms heretofore neglected or only indirectly included in other analyses. The experimental results showed that varying the characteristic length had negligible effect on performance, and that increasing the aspect ratio improved the performance in the transition region by producing a lower transition Reynolds number</p> <p>Two methods of controlling or preventing gas ingestion in viscoseals were studied. One, the centrifugal separator, sets up a circulating flow loop in the upper half of the viscoseal, sweeping gas bubbles from the annulus into an inner cavity where centrifugal action separates the gas from the liquid, which is returned to the annulus. Experimental results showed that the centrifugal separator reduced gas accumulation in the sealed cavity by an order of magnitude, and had negligible effect on sealing performance</p> <p>Another method of controlling gas ingestion involved a backflow of liquid from the high pressure region to the low pressure region of the viscoseal. Results showed that a backflow of suitable magnitude would effectively sweep out ingested gas and prevent its transport to the high pressure end of the viscoseal</p>			

